



Contents lists available at ScienceDirect

Journal of Traditional and Complementary Medicine

journal homepage: <http://www.elsevier.com/locate/jtcme>

Review article

# Anti-COVID-19 drug candidates: A review on potential biological activities of natural products in the management of new coronavirus infection



Anchalee Prasansuklab<sup>a</sup>, Atsadang Theerasri<sup>b</sup>, Panthakarn Rangsinth<sup>c</sup>,  
Chanin Sillapachaiyaporn<sup>b</sup>, Siriporn Chuchawankul<sup>c,d,\*\*</sup>, Tewin Tencomnao<sup>c,e,\*</sup>

<sup>a</sup> College of Public Health Sciences, Chulalongkorn University, Bangkok, 10330, Thailand

<sup>b</sup> Graduate Program in Clinical Biochemistry and Molecular Medicine, Department of Clinical Chemistry, Faculty of Allied Health Sciences, Chulalongkorn University, Bangkok, 10330, Thailand

<sup>c</sup> Immunomodulation of Natural Products Research Group, Faculty of Allied Health Sciences, Chulalongkorn University, Bangkok, 10330, Thailand

<sup>d</sup> Department of Transfusion Medicine and Clinical Microbiology, Faculty of Allied Health Sciences, Chulalongkorn University, Bangkok, 10330, Thailand

<sup>e</sup> Department of Clinical Chemistry, Faculty of Allied Health Sciences, Chulalongkorn University, Bangkok, 10330, Thailand

## ARTICLE INFO

### Article history:

Received 7 August 2020

Received in revised form

24 December 2020

Accepted 25 December 2020

Available online 29 December 2020

### Keywords:

SARS-CoV-2

2019-nCoV

Anti-viral

Therapeutic strategies

Natural compound

Herbal medicine

Plant

Mushroom

## ABSTRACT

**Background and aim:** The novel coronavirus disease (COVID-19) caused by severe acute respiratory syndrome coronavirus 2 (SARS-CoV-2) is now become a worldwide pandemic bringing over 71 million confirmed cases, while the specific drugs and vaccines approved for this disease are still limited regarding their effectiveness and adverse events. Since virus incidences are still on rise, infectivity and mortality may also rise in the near future, natural products are highly considered to be valuable sources for the discovery of new antiviral drugs against SARS-CoV-2. This present review aims to comprehensively summarize the up-to-date scientific literatures on biological activities of plant- and mushroom-derived compounds relevant to mechanistic targets involved in SARS-CoV-2 infection and inflammatory-associated pathogenesis, including viral entry, replication and release, and the renin-angiotensin-aldosterone system (RAAS).

**Experimental procedure:** Data were retrieved from a literature search available on PubMed, Scopus and Google Scholar databases and collected until the end of May 2020. The findings from *in vitro* cell and non-cell based studies were considered, while the results of *in silico* studies were excluded.

**Results and conclusion:** Based on the previous findings in SARS-CoV studies, except *in silico* molecular docking analysis, herein, we provide a total of 150 natural compounds as potential candidates for development of new anti-COVID-19 drugs with higher efficacy and lower toxicity than the existing therapeutic agents. Several natural compounds have showed their promising actions on multiple therapeutic targets, which should be further explored. Among them, quercetin, one of the most abundant of plant flavonoids, is proposed as a lead candidate with its ability on the virus side to inhibit SARS-CoV spike protein-angiotensin-converting enzyme 2 (ACE2) interaction, viral protease and helicase activities, as well as on the host cell side to inhibit ACE activity and increase intracellular zinc level.

© 2021 Center for Food and Biomolecules, National Taiwan University. Production and hosting by Elsevier Taiwan LLC. This is an open access article under the CC BY-NC-ND license (<http://creativecommons.org/licenses/by-nc-nd/4.0/>).

\* Corresponding author. Immunomodulation of Natural Products Research Group, Faculty of Allied Health Sciences, Chulalongkorn University, Bangkok, 10330, Thailand.

\*\* Corresponding author. Immunomodulation of Natural Products Research Group, Faculty of Allied Health Sciences, Chulalongkorn University, Bangkok, 10330, Thailand.  
E-mail addresses: [anchalee.pr@chula.ac.th](mailto:anchalee.pr@chula.ac.th) (A. Prasansuklab), [atsadang.the@gmail.com](mailto:atsadang.the@gmail.com) (A. Theerasri), [panthakarn.rangsinth@gmail.com](mailto:panthakarn.rangsinth@gmail.com) (P. Rangsinth), [chanin.sill@gmail.com](mailto:chanin.sill@gmail.com) (C. Sillapachaiyaporn), [siriporn.ch@chula.ac.th](mailto:siriporn.ch@chula.ac.th) (S. Chuchawankul), [tewin.t@chula.ac.th](mailto:tewin.t@chula.ac.th) (T. Tencomnao).

Peer review under responsibility of The Center for Food and Biomolecules, National Taiwan University.

**List of abbreviations**

3CL <sup>pro</sup>	3-chymotrypsin-like main protease
ACE	Angiotensin-converting enzyme
ARB	Angiotensin-receptor blocker
ARDS	Acute respiratory distress syndrome
AT1R	Angiotensin II type 1 receptor
COVID-19	Coronavirus Disease 2019
MERS-CoV	Middle East Respiratory Syndrome Coronavirus
Nsp	Non-structural protein
PL <sup>pro</sup>	Papain-like protease
RAAS	Renin–angiotensin–aldosterone system
RdRp	RNA-dependent RNA polymerase
RTC	Replication-transcription complex
SARS-CoV	Severe Acute Respiratory Syndrome Coronavirus
SARS-CoV-2	Severe Acute Respiratory Syndrome Coronavirus 2
TMPRSS2	Transmembrane protease serine 2
V-ATPase	Vacuolar-type H <sup>+</sup> -ATPase

**1. Introduction**

On 31 December 2019, several cases of pneumonia were reported in Wuhan, the epicenter of the outbreak in Hubei province of China.<sup>1</sup> The novel coronavirus was identified as Severe Acute Respiratory Syndrome Coronavirus 2 (SARS-CoV-2) which causes Coronavirus Disease 2019 (COVID-19) pandemic.<sup>2,3</sup> From the time of emergence until present, COVID-19 has spread worldwide in which a total of over 71 million confirmed cases with over 1.6 million death tolls has been reported by the World Health Organization (WHO). The COVID-19 positive cases continue rising and is widely distributed throughout the world with the prevalence ranging from highest in America, followed by Europe and South-East Asia, and lowest in Western Pacific region. Asymptomatic patients and patients with mild symptoms can be recovered under home care and isolation while patients with severe complications including acute respiratory distress syndrome (ARDS) require intensive care unit (ICU) which involves oxygen therapy.<sup>4,5</sup> Currently, there is scant evidence from clinical trials for WHO to approve any standard drugs or vaccines as several trials have failed due to efficacy and safety concerns.<sup>6,7</sup> Natural compounds from plant and fungi sources have been recognized in their antiviral properties with numerous mechanisms to prevent infection and strengthen host immunity.<sup>8,9</sup> Herein, we reviewed potential antiviral compounds with multiple targets of action relating to coronaviruses including inhibiting of viral entry, replication and release, and compounds targeting renin–angiotensin–aldosterone system (RAAS) which exhibit promising effects against the disease. We also proposed future perspectives in adopting natural compounds to combat against the COVID-19.

**2. Promising therapeutic strategies for the treatment of COVID-19 infection**

Presently, there is no clinically approved therapeutics for treating COVID-19, while the rapid human-to-human transmission of this viral infection has expanded worldwide. As the efficacy and safety of natural products on the treatment of a number of viruses including SARS-CoV and Middle East Respiratory Syndrome Coronavirus (MERS-CoV), have been widely acknowledged for several years,<sup>10</sup> the compounds derived from natural sources, e.g. plants and fungi, could have the potential to be a powerful anti-COVID-19

drug. In this review, we focused on four main categories of therapeutic strategies that aim to target the cellular machinery at each step of virus life cycle, starting from viral entry and replication to the release of viral progenies, as well as the RAAS which is a main target of the treatment of hypertension and has recently been proposed as another promising alternative in the treatment of COVID-19. The multiple potential therapeutic mechanisms, both specific and general, that could be capable of tackling COVID-19 infection are presented in Fig. 1.

The first therapeutic strategy targets on the mechanisms of virus entry in which the selective blockade of molecules that facilitates the internalization of virus into the host cells could be effective to prevent infection. Upon the binding of a virus surface spike (S) protein to a cellular receptor angiotensin-converting enzyme 2 (ACE2), the SARS-CoV-2 generally enters into target host cells via two primary routes; viral membrane fusion and the more common endocytic uptake.<sup>11</sup> The first entry mechanism is assisted by proteolytic activation of S protein by a host cell transmembrane protease serine 2 (TMPRSS2), which allows not only direct fusion of virus at the plasma membrane surface, but also release of viral genomic RNA into the cytoplasm. On the other hand, without the membrane bound protease TMPRSS2, the latter entry mechanism allows the whole viral particle to be uptaken via receptor-mediated endocytosis, before subsequently uncoated following the S protein cleavage by cathepsin L within the endosome, to unveil its RNA genome into the cell.

The second and third therapeutic strategies focus on the inhibition of progeny virus production and release from infected cells. As far as the viral replication process is concerned,<sup>12</sup> it begins with the translation of released genome of SARS-CoV-2, a single-stranded (positive-sense) RNA of approximately 30 kb in length, into two precursor polyproteins, pp1a and pp1ab. Both are further cleaved by virus-encoded proteases into several non-structural proteins (nsps) including two key replicative enzymes: the nsp12-RNA-dependent RNA polymerase (RdRp) and the nsp13-helicase, to form the replication-transcription complex (RTC) for synthesizing a full-length genomic RNA (replication) or a nested set of subgenomic mRNA (transcription). These mRNAs are translated into all relevant structural proteins, which together with the viral genome are subsequently assembled into new virions and finally released outside the cell through viroporin-mediated viral budding.<sup>13</sup>

The last therapeutic strategy involves modulating the immune system with the RAAS which regulates blood pressure, fibrosis, and inflammation. In this system, angiotensin-converting enzyme (ACE) converts angiotensin I to angiotensin II which is then converted to lung-protective angiotensin-(1–7) by ACE2. The angiotensin-(1–7) is further recognized by its receptor, the G-protein coupled receptor Mas, to reduce blood pressure, fibrosis, and inflammation.<sup>14</sup> However, as SARS-CoV-2 enters the cells by binding to ACE2, the normal functions of ACE2 are then suppressed. Therefore, instead of converting to angiotensin-(1–7), the angiotensin II is largely bound to type 1 angiotensin II type 1 receptor (AT1R) which causing increased inflammation and other deleterious effects, particularly in the renal and cardiovascular systems.<sup>15</sup>

**3. Potential natural products as drug candidates against COVID-19**

The data presented in this review were obtained from PubMed, Scopus and Google Scholar database up to May 2020. The terms of natural compound, natural product, plant and mushroom were individually searched along with the terms corresponding to each target molecule. Here, we summarize plant- and mushroom-derived compounds that have been reported of antiviral activity

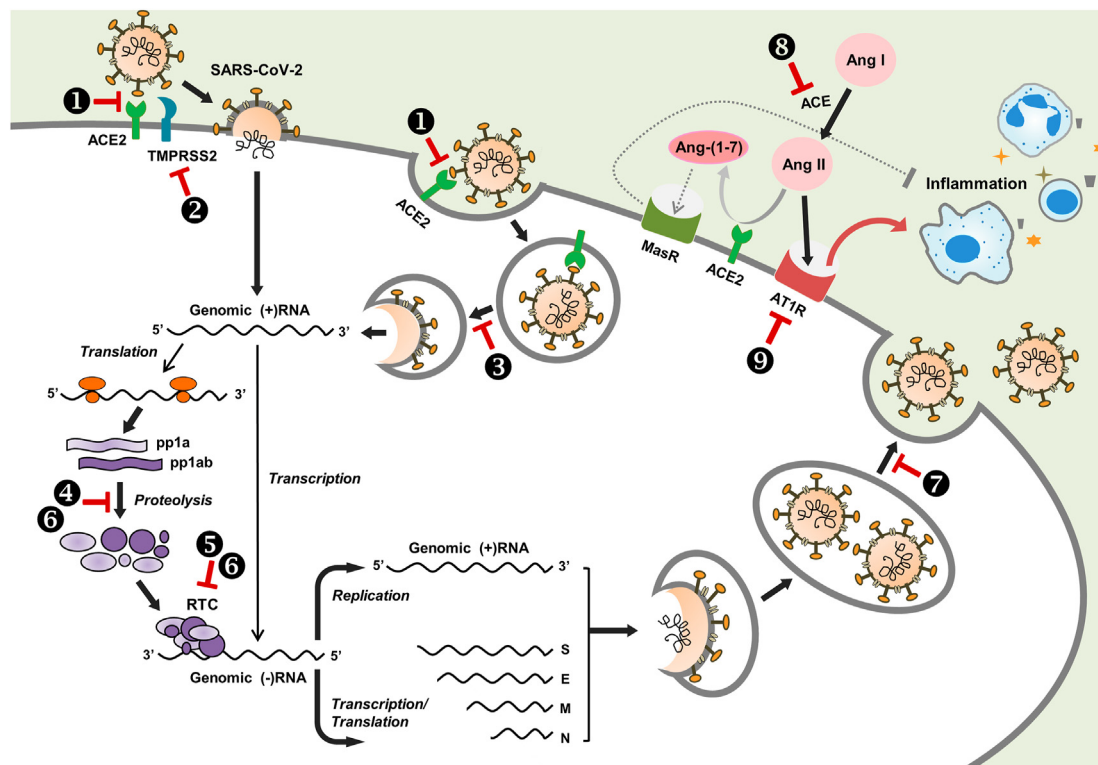


**Fig. 1.** Schematic illustration of potential therapeutic mechanisms in COVID-19 infection. The potential therapeutic strategies for SARS-CoV-2 infection proposed here fall into four main categories based on the cellular and molecular machinery required for the viral life cycle and its related pathogenic mechanisms: inhibition of virus entry, inhibition of virus replication, blocking the release of viral progenies, and modifying the RAAS. The selective blockade of the S protein-ACE2 binding (1), TMPRSS2 activity (2), and endocytic pathway-associated proteins such as clathrin, the vacuolar-type H<sup>+</sup>-ATPase (V-ATPase), and cathepsin L (3), prevent the internalization of virus within the cell. Virus multiplication can be blocked through direct inhibition of proteolytic activity of two viral proteases, 3CL<sup>pro</sup> and PL<sup>pro</sup> (4), and replicative activity of viral RTC components e.g., RdRp and helicase (5), or indirect enzyme inhibition by increasing intracellular Zn<sup>2+</sup> concentration (6). Silencing the expression and ion channel activity of viroporin 3a suppresses the release of viral particles from infected cells (7). Overactivation of Ang II/AT1R axis which contributes to excessive inflammation, can be suppressed by blockade of ACE (8) and AT1R (9). 3CL<sup>pro</sup>, 3-chymotrypsin-like protease; ACE2, angiotensin-converting enzyme 2; Ang I, angiotensin; AT1R, angiotensin II type 1 receptor; E, envelope; MasR, mitochondrial assembly receptor; M, membrane; N, nucleocapsid; PL<sup>pro</sup>, papain-like protease; pp, polyprotein; RAAS, renin-angiotensin-aldosterone system; RdRp, RNA-dependent RNA polymerase; RTC, replication-transcription complex; S, spike; TMPRSS2, transmembrane protease serine 2.

with known therapeutic mechanisms specifically against SARS-CoV infection, performed by *in vitro* cell or non-cell based experiments but not *in silico* method, as potential candidates to be further researched. We also propose certain promising natural compounds targeting general mechanisms involved in coronavirus infection (see Fig. 1). Additionally, the reports on natural compounds against SARS-CoV with unidentified mechanism of action were included in this review.

### 3.1. Natural bioactive compounds targeting viral entry

#### 3.1.1. The S protein-ACE2 interaction

The S protein plays a pivotal role in the entry of coronaviruses into host cells by recognizing and binding to the ACE2 via multivalent bonds.<sup>16</sup> The attachment of S protein to ACE2 receptor leads to the fusion between the viral envelope and host cell membrane resulting in successful transfer of viral genome into infected cells.<sup>17,18</sup> S protein is composed of two functional subunits, S1 and S2. The S1 is responsible for binding to the host cell receptor through the receptor binding domain (RBD), while the S2 causes fusion of the viral and cellular membranes.<sup>19,20</sup> Sequence alignment results showed that the homology of the S protein RBD sequence between the beta coronaviruses SARS-CoV and SARS-CoV-2 is 76%.<sup>21</sup> A number of evidence revealed human ACE2 (hACE2) molecule as an entry receptor for both SARS-CoV and SARS-CoV-2 S proteins.<sup>22–25</sup> Notably, S protein of SARS-CoV-2 was found to

exhibit greater affinity to the ACE2 receptor than that of SARS-CoV.<sup>24</sup> In addition, expression of ACE2 is ubiquitous with diverse functions, however its specific functions are demonstrated in several organs including lung, tongue, heart, kidney, gastrointestinal tract, pancreas and brain.<sup>26,27</sup> Accordingly, multiple symptoms could be observed in COVID-19 patients.<sup>27</sup> Several observations have been reported that the use of hydroxychloroquine, an ACE2 FDA-approved antagonist, was able to reduce mortality rate in hospitalized COVID-19 patients.<sup>28</sup> Therefore, it is apparent that the S protein-hACE2 interaction complex is the most crucial target for searching appropriate inhibitors to inhibit entry of the virus in the host cell.

Several natural compounds have been demonstrated their activity to inhibit SARS-CoV entry to the host cell as shown in Table 1. According to the literature, an anthraquinone compound, emodin, showed the potency to inhibit viral infection by blocking the binding of SARS-CoV S protein to ACE2 in a dose-dependent manner.<sup>29</sup> The plant sources which are likely to contain emodin as their active constituent were also found effective in blocking SARS-CoV S protein and ACE2 interaction, with showing IC<sub>50</sub> values for aqueous extracts from the root of *Rheum palmatum*, the root and stem of *Polygonum multiflorum*, ranged from 1 to 10 µg/ml.<sup>29</sup> Another previous study using the high-throughput screening technique revealed more promising natural antiviral compounds consisted in the extracts from Chinese herbs. Those small herbal molecules could strongly bind to the SARS-CoV S2 protein and

**Table 1**

List of bioactive compounds from natural sources as potential anti-COVID-19 drug candidates and their mechanisms of action.

Compound	Class	Source	Biological action/Efficacy	Experiment	Reference
<b>Inhibiting the SARS-CoV S protein-ACE2 interaction</b>					
Emodin	Anthraquinone	<i>Rheum palmatum</i> <sup>a</sup>	IC <sub>50</sub> = 200 μM	Cell-free assay (Competitive biotinylated ELISA)	29
Luteolin	Flavonoid	<i>Rhodiola kirilowii</i> <sup>a</sup>	94% inhibition at EC of 50 μM IC <sub>50</sub> = 4.5 μM	Cell-based assay (IFA)	30
Quercetin	Flavonoid	<i>Allium cepa</i> <sup>a</sup>	IC <sub>50</sub> = 83.4 μM	Cell-free and cell-based assay (FAC/MS and Luciferase assay)	30
Tetra-O-galloyl-β-D-glucose (TGG)	Tannin	<i>Galla chinensis</i> <sup>a</sup>	IC <sub>50</sub> = 10.6 μM	Cell-based assay (Luciferase assay)	30
<b>Inhibiting the endocytic machinery</b>					
1-cinnamoyl-3,11-dihydroxy meliacarpin	Terpenoid	<i>Melia azedarach</i>	increased endolysosomal pH (EC of 7.5 μM)	Cell-based assay (AO staining)	38
25-O-acetyl-7,8-didehydrocimigenol 3-O-beta-D-xylopyranoside (ADCX)	Terpenoid	<i>Cimicifugae rhizoma</i>	inhibited degradation activity by decreasing cathepsin expression, but not endolysosomal acidity (EC of 24 μM)	Cell-based assay (AO staining, DQ-BSA staining and WB)	39
Alantolactone	Sesquiterpene lactone	<i>Inula helenium</i> <sup>a</sup>	neutralized endo-lysosomal pH and reducing the expression and activity of cathepsins (EC of 10 μM)	Cell-based assay (LysoTracker Red and AO staining, WB and Cathepsin activity assay)	76
Cleistanthin A	Lignan glycoside	<i>Cleistanthus collinu</i> <sup>a</sup>	inhibited the activity of V-type ATPase and elevated endolysosomal pH (EC of 0.1 μM)	Cell-based assay (pH sensitive fluorescent probe/LysoTracker Red staining and V-type ATPase activity assay)	77,78
Cleistanthoside A tetraacetate	Lignan glycoside	<i>Phyllanthus taxodiifolius</i> <i>Beille</i> <sup>a</sup>	neutralized endolysosomal acidity and decreased the activity of V-type ATPase (EC of 50 nM)	Cell-based assay (LysoTracker Red staining and V-type ATPase activity assay)	78
Dauricine	Alkaloid	<i>Rhizoma Menisperm</i> <sup>a</sup>	elevated endolysosomal pH, decreased the levels of active cathepsins and inhibited the activity of V-type ATPase (EC of 10 μM)	Cell-based assay (LysoSensor Yellow/Blue staining, WB and V-type ATPase activity assay)	42
Daurisolone	Alkaloid	<i>Rhizoma Menisperm</i> <sup>a</sup>	elevated endolysosomal pH, decreased the levels of active cathepsins and inhibited the activity of V-type ATPase (EC of 10 μM)	Cell-based assay (LysoSensor Yellow/Blue staining, WB and V-type ATPase activity assay)	42
Diphyllin	Lignan lactone	<i>Cleistanthus collinus</i> <sup>a</sup>	inhibited the activity of V-type ATPase (EC of 0.3 μM)	Cell-based assay (V-type ATPase activity assay)	79
Ginsenoside Ro	Triterpenoid saponin	<i>Panax ginseng</i>	raised endolysosomal pH and downregulating the expression and activity of cathepsins (EC of 50 μM)	Cell-based assay (AO staining, WB and Cathepsin activity assay)	80
Icariside II	Flavonoid	<i>Epimedium koreanum</i> Nakai	decreased endolysosomal acidity (EC of 25 μM)	Cell-based assay (AO staining)	81
Leelamine	Terpene	<i>Pinus sylvestris</i> <sup>a</sup>	decreased endolysosomal acidity and inhibited cellular endocytosis (EC of 3 μM)	Cell-based assay (LysoTracker Red staining and Internalization of fluorescent transferrin-A488)	40
Matrine	Alkaloid	<i>Sophora flavescens</i> Ait	inhibited endolysosomal acidification and reduced the expression and activity of cathepsins (EC of 2 mM)	Cell-based assay (LysoSensor Yellow/Blue, WB and Cathepsin activity assay)	43
Myrtenal	Terpene	<i>Elettaria cardamomum</i> <sup>a</sup>	inhibited the activity of V-type ATPase and reduced endolysosomal acidification (EC of 100 μM)	Cell-based assay (AO staining and V-type ATPase activity assay)	41
Oblongifolin C	Benzophenone	<i>Garcinia yunnanensis</i> Hu	inhibited endolysosomal acidification and downregulated the expression and activity of cathepsins (EC of 15 μM)	Cell-based assay (AO staining, WB and Cathepsin activity assay)	82
Pulsatilla saponin D	Triterpenoid saponin	<i>Pulsatilla chinensis</i> (Bunge) Regel	elevated endolysosomal pH and downregulated cathepsins (EC of 1.25 μM)	Cell-based assay (LysoSensor Yellow/Blue, WB and Cathepsin activity assay)	83
Tetrandrine	Alkaloid	<i>Stephania tetrandra</i> S. Moore <sup>a</sup>	elevated endolysosomal pH in a concentration-dependent manner (EC of 1–10 μM)	Cell-based assay (LysoSensor Yellow/Blue staining)	44
<b>Inhibiting the SARS-CoV 3CL<sup>pro</sup> activity</b>					
3'-(3-Methylbut-2-enyl)-3',4,7-trihydroxyflavane	Flavonoid	<i>Broussonetia papyrifera</i>	IC <sub>50</sub> = 30.2 μM	Cell-free assay (FRET)	84
4-Hydroxyderricin	Chalcone	<i>Angelica keiskei</i>	IC <sub>50</sub> = 81.4 μM IC <sub>50</sub> = 50.8 μM	Cell-free assay (FRET) Cell-based assay (Luciferase reporter assay)	35
Betulinic acid	Terpenoid	<i>Breynia fruticose</i> <sup>a</sup>	IC <sub>50</sub> = 10 μM	Cell-free assay (FRET)	49,50
Brousochalcone A	Chalcone	<i>Broussonetia papyrifera</i>	IC <sub>50</sub> = 88.1 μM	Cell-free assay (FRET)	84
Brousochalcone B	Chalcone	<i>Broussonetia papyrifera</i>	IC <sub>50</sub> = 57.8 μM	Cell-free assay (FRET)	84
Brousoflavan A	Flavonoid	<i>Broussonetia papyrifera</i>	IC <sub>50</sub> = 92.4 μM	Cell-free assay (FRET)	84
Dihydrotanshinone I	Tanshinone	<i>Salvia miltiorrhiza</i>	IC <sub>50</sub> = 14.4 μM	Cell-free assay (FRET)	51
Hesperetin	Flavonoid	<i>Isatis indigotica</i>	IC <sub>50</sub> = 60 μM	Cell-free assay (ELISA)	48

(continued on next page)



Table 1 (continued)

Compound	Class	Source	Biological action/Efficacy	Experiment	Reference
			IC <sub>50</sub> = 8.3 μM	Cell-based assay (Luciferase reporter assay)	
Hirsutenone	Diarylheptanoid	<i>Alnus japonica</i>	IC <sub>50</sub> = 36.2 μM	Cell-free assay (FRET)	85
Isobavachalcone	Chalcone	<i>Angelica keiskei</i>	IC <sub>50</sub> = 39.4 μM IC <sub>50</sub> = 11.9 μM	Cell-free assay (FRET) Cell-based assay (Luciferase reporter assay)	35
Isoliquiritigenin	Chalcone	<i>Glycyrrhiza glabra</i> <sup>a</sup>	IC <sub>50</sub> = 61.9 μM	Cell-free assay (FRET)	84,86
Kazinol A	Flavonoid	<i>Broussonetia papyrifera</i>	IC <sub>50</sub> = 84.8 μM	Cell-free assay (FRET)	84
Kazinol F	Biphenyl propanoids	<i>Broussonetia papyrifera</i>	IC <sub>50</sub> = 43.3 μM	Cell-free assay (FRET)	84
Kazinol J	Biphenyl propanoids	<i>Broussonetia papyrifera</i>	IC <sub>50</sub> = 64.2 μM	Cell-free assay (FRET)	84
Methyl tanshinonate	Tanshinone	<i>Salvia miltiorrhiza</i>	IC <sub>50</sub> = 21.1 μM	Cell-free assay (FRET)	51
Quercetin	Flavonoid	<i>Allium cepa</i> <sup>a</sup>	IC <sub>50</sub> = 52.7 μM	Cell-free assay (FRET)	84,87
Quercetin-3-b-galactoside	Flavonoid	<i>Machilus zuihoensis</i> <sup>a</sup>	IC <sub>50</sub> = 42.8 μM	Cell-free assay (FRET)	87,88
Rosmariquinone	Tanshinone	<i>Salvia miltiorrhiza</i>	IC <sub>50</sub> = 21.1 μM	Cell-free assay (FRET)	51
Savinin	Lignoid	<i>Chamaecyparis obtuse</i> var. <i>formosana</i>	IC <sub>50</sub> = 25 μM	Cell-free assay (FRET)	49
Tanshinone I	Tanshinone	<i>Salvia miltiorrhiza</i>	IC <sub>50</sub> = 38.7 μM	Cell-free assay (FRET)	51
Tanshinone IIA	Tanshinone	<i>Salvia miltiorrhiza</i>	IC <sub>50</sub> = 89.1 μM	Cell-free assay (FRET)	51
Tanshinone IIB	Tanshinone	<i>Salvia miltiorrhiza</i>	IC <sub>50</sub> = 24.8 μM	Cell-free assay (FRET)	51
Xanthoangelol	Chalcone	<i>Angelica keiskei</i>	IC <sub>50</sub> = 38.4 μM IC <sub>50</sub> = 5.8 μM	Cell-free assay (FRET) Cell-based assay (Luciferase reporter assay)	35
Xanthoangelol B	Chalcone	<i>Angelica keiskei</i>	IC <sub>50</sub> = 22.2 μM IC <sub>50</sub> = 8.6 μM	Cell-free assay (FRET) Cell-based assay (Luciferase reporter assay)	35
Xanthoangelol D	Chalcone	<i>Angelica keiskei</i>	IC <sub>50</sub> = 26.6 μM IC <sub>50</sub> = 9.3 μM	Cell-free assay (FRET) Cell-based assay (Luciferase reporter assay)	35
Xanthoangelol E	Chalcone	<i>Angelica keiskei</i>	IC <sub>50</sub> = 11.4 μM IC <sub>50</sub> = 7.1 μM	Cell-free assay (FRET) Cell-based assay (Luciferase reporter assay)	35
Xanthoangelol F	Chalcone	<i>Angelica keiskei</i>	IC <sub>50</sub> = 34.1 μM IC <sub>50</sub> = 32.6 μM	Cell-free assay (FRET) Cell-based assay (Luciferase reporter assay)	35
Xanthokeistal A	Chalcone	<i>Angelica keiskei</i>	IC <sub>50</sub> = 44.1 μM IC <sub>50</sub> = 9.8 μM	Cell-free assay (FRET) Cell-based assay (Luciferase reporter assay)	35
<b>Inhibiting the SARS-CoV PLP<sup>pro</sup> activity</b>					
3'-O-Methyl diplacol	Flavonoid	<i>Paulownia tomentosa</i>	IC <sub>50</sub> = 9.5 μM	Cell-free assay (Fluorescence-based deubiquitination)	89
3'-O-Methyl diplacone	Flavonoid	<i>Paulownia tomentosa</i>	IC <sub>50</sub> = 13.2 μM	Cell-free assay (Fluorescence-based deubiquitination)	89
4'-O-Methylbavachalcone	Chalcone	<i>Psoralea corylifolia</i>	IC <sub>50</sub> = 10.1 μM	Cell-free assay (Fluorescence-based deubiquitination)	90
4'-O-Methyl diplacol	Flavonoid	<i>Paulownia tomentosa</i>	IC <sub>50</sub> = 9.2 μM	Cell-free assay (Fluorescence-based deubiquitination)	89
4'-O-Methyl diplacone	Flavonoid	<i>Paulownia tomentosa</i>	IC <sub>50</sub> = 12.7 μM	Cell-free assay (Fluorescence-based deubiquitination)	89
6-Geranyl-4',5,7-trihydroxy-3',5'-dimethoxyflavanone	Flavonoid	<i>Paulownia tomentosa</i>	IC <sub>50</sub> = 13.9 μM	Cell-free assay (Fluorescence-based deubiquitination)	89
Brousochalcone A	Chalcone	<i>Broussonetia papyrifera</i>	IC <sub>50</sub> = 9.2 μM	Cell-free assay (Fluorescence-based deubiquitination)	84
Brousochalcone B	Chalcone	<i>Broussonetia papyrifera</i>	IC <sub>50</sub> = 11.6 μM	Cell-free assay (Fluorescence-based deubiquitination)	84
Cryptotanshinone	Tanshinone	<i>Salvia miltiorrhiza</i>	IC <sub>50</sub> = 0.8 μM	Cell-free assay (Fluorescence-based deubiquitination)	51
Curcumin	Polyphenol	<i>Curcuma longa</i> <sup>a</sup>	IC <sub>50</sub> = 5.7 μM	Cell-free assay (Fluorescence-based deubiquitination)	85,91
Dihydrotanshinone I	Tanshinone	<i>Salvia miltiorrhiza</i>	IC <sub>50</sub> = 4.9 μM	Cell-free assay (Fluorescence-based deubiquitination)	51
Diplacone	Flavonoid	<i>Paulownia tomentosa</i>	IC <sub>50</sub> = 10.4 μM	Cell-free assay (Fluorescence-based deubiquitination)	89
Hirsutanonol	Diarylheptanoid	<i>Alnus japonica</i>	IC <sub>50</sub> = 7.8 μM	Cell-free assay (Fluorescence-based deubiquitination)	85

Table 1 (continued)

Compound	Class	Source	Biological action/Efficacy	Experiment	Reference
Hirsutenone	Diarylheptanoid	<i>Alnus japonica</i>	IC <sub>50</sub> = 4.1 μM	Cell-free assay (Fluorescence-based deubiquitination)	85
Isobavachalcone	Chalcone	<i>Psoralea corylifolia</i> <i>Angelica keiskei</i>	IC <sub>50</sub> = 7.3 μM IC <sub>50</sub> = 13.0 μM	Cell-free assay (Fluorescence-based deubiquitination)	90 35
Isoliquiritigenin	Chalcone	<i>Glycyrrhiza glabra</i> <sup>a</sup>	IC <sub>50</sub> = 24.6 μM	Cell-free assay (Fluorescence-based deubiquitination)	84,86
Kaempferol	Flavonoid	<i>Zingiber officinale</i> <sup>a</sup>	IC <sub>50</sub> = 16.3 μM	Cell-free assay (Fluorescence-based deubiquitination)	84,92
Kazinol J	Biphenyl propanoids	<i>Broussonetia papyrifera</i>	IC <sub>50</sub> = 15.2 μM	Cell-free assay (Fluorescence-based deubiquitination)	84
Methyl tanshinonate	Tanshinone	<i>Salvia miltiorrhiza</i>	IC <sub>50</sub> = 9.2 μM	Cell-free assay (Fluorescence-based deubiquitination)	51
Mimulone	Flavonoid	<i>Paulownia tomentosa</i>	IC <sub>50</sub> = 14.4 μM	Cell-free assay (Fluorescence-based deubiquitination)	89
Neobavaisoflavone	Flavonoid	<i>Psoralea corylifolia</i>	IC <sub>50</sub> = 18.3 μM	Cell-free assay (Fluorescence-based deubiquitination)	90
Papyriflavonol A	Favonoid	<i>Broussonetia papyrifera</i>	IC <sub>50</sub> = 3.7 μM	Cell-free assay (Fluorescence-based deubiquitination)	84
Psoralidin	Flavonoid	<i>Psoralea corylifolia</i>	IC <sub>50</sub> = 4.2 μM	Cell-free assay (Fluorescence-based deubiquitination)	90
Quercetin	Flavonoid	<i>Allium cepa</i> <sup>a</sup>	IC <sub>50</sub> = 8.6 μM	Cell-free assay (Fluorescence-based deubiquitination)	84,87
Rubranol	Diarylheptanoid	<i>Alnus japonica</i>	IC <sub>50</sub> = 12.3 μM	Cell-free assay (Fluorescence-based deubiquitination)	85
Rubranoside A	Diarylheptanoid	<i>Alnus japonica</i>	IC <sub>50</sub> = 9.1 μM	Cell-free assay (Fluorescence-based deubiquitination)	85
Rubranoside B	Diarylheptanoid	<i>Alnus japonica</i>	IC <sub>50</sub> = 8.0 μM	Cell-free assay (Fluorescence-based deubiquitination)	85
Tanshinone I	Tanshinone	<i>Salvia miltiorrhiza</i>	IC <sub>50</sub> = 8.8 μM	Cell-free assay (Fluorescence-based deubiquitination)	51
Tanshinone IIA	Tanshinone	<i>Salvia miltiorrhiza</i>	IC <sub>50</sub> = 1.6 μM	Cell-free assay (Fluorescence-based deubiquitination)	51
Tanshinone IIB	Tanshinone	<i>Salvia miltiorrhiza</i>	IC <sub>50</sub> = 10.7 μM	Cell-free assay (Fluorescence-based deubiquitination)	51
Terrestriamine	Cinnamic amide	<i>Tribulus terrestris</i>	IC <sub>50</sub> = 15.8 μM	Cell-free assay (Fluorescence-based deubiquitination)	93
Tomentin A	Flavonoid	<i>Paulownia tomentosa</i>	IC <sub>50</sub> = 6.2 μM	Cell-free assay (Fluorescence-based deubiquitination)	89
Tomentin B	Flavonoid	<i>Paulownia tomentosa</i>	IC <sub>50</sub> = 6.1 μM	Cell-free assay (Fluorescence-based deubiquitination)	89
Tomentin C	Flavonoid	<i>Paulownia tomentosa</i>	IC <sub>50</sub> = 11.6 μM	Cell-free assay (Fluorescence-based deubiquitination)	89
Tomentin D	Flavonoid	<i>Paulownia tomentosa</i>	IC <sub>50</sub> = 12.5 μM	Cell-free assay (Fluorescence-based deubiquitination)	89
Tomentin E	Flavonoid	<i>Paulownia tomentosa</i>	IC <sub>50</sub> = 5.0 μM	Cell-free assay (Fluorescence-based deubiquitination)	89
Xanthoangelol	Chalcone	<i>Angelica keiskei</i>	IC <sub>50</sub> = 11.7 μM	Cell-free assay (Fluorescence-based deubiquitination)	35
Xanthoangelol B	Chalcone	<i>Angelica keiskei</i>	IC <sub>50</sub> = 11.7 μM	Cell-free assay (Fluorescence-based deubiquitination)	35
Xanthoangelol D	Chalcone	<i>Angelica keiskei</i>	IC <sub>50</sub> = 19.3 μM	Cell-free assay (Fluorescence-based deubiquitination)	35
Xanthoangelol E	Chalcone	<i>Angelica keiskei</i>	IC <sub>50</sub> = 1.2 μM	Cell-free assay (Fluorescence-based deubiquitination)	35
Xanthoangelol F	Chalcone	<i>Angelica keiskei</i>	IC <sub>50</sub> = 5.6 μM	Cell-free assay (Fluorescence-based deubiquitination)	35
<b>Inhibiting the SARS-CoV helicase activity</b>					
Myricetin	Flavonoid	<i>Camellia sinensis</i> <sup>a</sup>	inhibited ATPase activity of SARS-CoV helicase with IC <sub>50</sub> of 2.71 μM	Cell-free assay (Colorimetry-based ATP hydrolysis assay)	94
Quercetin	Flavonoid	<i>Allium cepa</i> <sup>a</sup>	inhibited duplex DNA-unwinding activity of SARS-CoV NTPase/helicase with IC <sub>50</sub> of 8.1 μM	Cell-free assay (FRET-based dsDNA unwinding assay)	95
Scutellarein	Flavonoid glycoside	<i>Scutellaria baicalensis</i>	inhibited ATPase activity of SARS-CoV helicase with IC <sub>50</sub> of 0.86 μM	Cell-free assay (Colorimetry-based ATP hydrolysis assay)	94
<b>Increasing intracellular Zn<sup>2+</sup></b>					
Caffeic acid	Phenolic acid	<i>Ocimum basilicum</i> <sup>a</sup>	increased intracellular Zn <sup>2+</sup> level (3-fold increase at EC of 50 μM)	Cell-free assay (using liposome model)	60
Catechin	Flavonoid	<i>Camellia sinensis</i> <sup>a</sup>	increased intracellular Zn <sup>2+</sup> level (2-fold increase at EC of 50 μM)	Cell-free assay (using liposome model)	60
Catechol	Phenol	<i>Allium cepa</i> <sup>a</sup>	increased intracellular Zn <sup>2+</sup> level (2-fold increase at EC of 50 μM)	Cell-free assay (using liposome model)	60
Epigallocatechin-3-gallate (EGCG)	Flavonoid	<i>Camellia sinensis</i> <sup>a</sup>	increased intracellular Zn <sup>2+</sup> level (36-fold increase at EC of 50 μM)	Cell-free assay (using liposome model)	60

(continued on next page)

Table 1 (continued)

Compound	Class	Source	Biological action/Efficacy	Experiment	Reference
Gallic acid	Phenolic acid	<i>Syzygium aromaticum</i> <sup>a</sup>	increased the uptake of Zn <sup>2+</sup> in both cell (4-fold increase at EC of 100 μM) and liposome model (16-fold increase at EC of 10 μM)	Cell-based assay (Fluorescent Zn <sup>2+</sup> indicator) and cell-free assay (using liposome model)	62
Genistein	Flavonoid	<i>Glycine max</i> <sup>a</sup>	increased intracellular Zn <sup>2+</sup> level (8-fold increase at EC of 50 μM)	Cell-free assay (using liposome model)	60
Luteolin	Flavonoid	<i>Rhodiola kirilowii</i> <sup>a</sup>	increased intracellular Zn <sup>2+</sup> level (12-fold increase at EC of 50 μM)	Cell-free assay (using liposome model)	60
Pyrithione	Organic sulfur compound	<i>Allium stipitatum</i> <sup>a</sup>	increased intracellular Zn <sup>2+</sup> level (3-fold increase at EC of 10 μM)	Cell-based assay (Radioactive Zn <sup>2+</sup> uptake)	96
Quercetin	Flavonoid	<i>Allium cepa</i> <sup>a</sup>	increased intracellular Zn <sup>2+</sup> level (18-fold increase at EC of 50 μM)	Cell-free assay (using liposome model)	60
Resveratrol	Polyphenol	<i>Vitis vinifera</i> <sup>a</sup>	increased the uptake of Zn <sup>2+</sup> in both cell (2-fold increase at EC of 100 μM) and liposome model (8-fold increase at EC of 10 μM)	Cell-based assay (Fluorescent Zn <sup>2+</sup> indicator) and cell-free assay (using liposome model)	[62]
Rutin	Flavonoid glycoside	<i>Morus alba</i> <sup>a</sup>	increased intracellular Zn <sup>2+</sup> level (7.5-fold increase at EC of 10 μM)	Cell-based assay (AAS)	61
Tannic acid	Phenolic acid	<i>Camellia sinensis</i> <sup>a</sup>	increased intracellular Zn <sup>2+</sup> level (4-fold increase at EC of 50 μM)	Cell-free assay (using liposome model)	60
Taxifolin	Flavonoid	<i>Silybum marianum</i> <sup>a</sup>	increased intracellular Zn <sup>2+</sup> level (12-fold increase at EC of 50 μM)	Cell-free assay (using liposome model)	60
β-thujaplicin (Hinokitiol)	Terpene	<i>Chamaecyparis obtusa</i> <sup>a</sup>	increased intracellular Zn <sup>2+</sup> level (4-fold increase at EC of 50 μM)	Cell-free assay (using liposome model)	60
<b>Inhibiting the viroporin 3a activity</b>					
Afzelin	Flavonoid glycoside	<i>Houttuynia cordata</i> <sup>a</sup>	increased intracellular Zn <sup>2+</sup> level (3-fold increase at EC of 125 μM)	Cell-based assay (Radioactive Zn <sup>2+</sup> uptake)	96
Emodin	Anthraquinone	<i>Rheum tanguticum</i>	inhibited the ion channel activity of SARS-CoV 3a protein (17% inhibition at EC of 10 μM)	Cell-based assay (Voltage-clamp method in Xenopus oocyte model)	65
Juglanine	Flavonoid glycoside	<i>Polygonum aviculare</i> <sup>a</sup>	inhibited the ion channel activity of SARS-CoV 3a protein with IC <sub>50</sub> of 2.3 μM	Cell-based assay (Voltage-clamp method in Xenopus oocyte model)	66,97
Kaempferol	Flavonoid	<i>Zingiber officinale</i> <sup>a</sup>	inhibited the ion channel activity of SARS-CoV 3a protein with IC <sub>50</sub> of 2.3 μM	Cell-based assay (Voltage-clamp method in Xenopus oocyte model)	65
Kaempferol-3-O-α-rhamnopyranosyl (1 → 2) [α-rhamno pyranosyl(1 → 6)]-β-glucopyranoside	Flavonoid glycoside	<i>Clitoria ternatea</i> <sup>a</sup>	inhibited the ion channel activity of SARS-CoV 3a protein (18% inhibition at EC of 20 μM)	Cell-based assay (Voltage-clamp method in Xenopus oocyte model)	65,66
Tiliroside	Flavonoid glycoside	<i>Althaea officinalis</i> <sup>a</sup>	inhibited the ion channel activity of SARS-CoV 3a protein (32% inhibition at EC of 20 μM)	Cell-based assay (Voltage-clamp method in Xenopus oocyte model)	65
<b>Inhibiting the ACE activity</b>					
25-O-methylalisol F	Triterpenoid	<i>Alisma orientale</i>	Reduced ACE and AT1R protein expression (~30% and ~10% inhibition at EC of 10 μM)	Cell-based assay (WB analysis)	98
3,5-dihydroxy-4- methoxybenzoic acid	Phenolic acid	<i>Tamarix hohenackeri</i>	46.2% inhibition at EC of 20 mg/mL	Cell-free assay (HHL degradation assay)	99
4'-hydroxy Pd-C-III	Coumarin	<i>Angelica decursiva</i>	IC <sub>50</sub> = 9.4 μM	Cell-free assay (FAPGG degradation assay)	100
4'-methoxy Pd-C-I	Coumarin	<i>Angelica decursiva</i>	IC <sub>50</sub> = 16 μM	Cell-free assay (FAPGG degradation assay)	100
Ampleopsin C	Stilbenoid	<i>Vitis thunbergii</i> var. <i>Taiwanian</i>	IC <sub>50</sub> = 18.2 μM	Cell-free assay (FAPGG degradation assay)	101
Apigenin	Flavonoid	<i>Adinandra nitida</i> <sup>a</sup>	30.3% inhibition at EC of 500 μg/mL	Cell-free assay (HHL degradation assay)	102
Asparaptine	Organic sulfur compound	<i>Asparagus officinalis</i>	IC <sub>50</sub> = 113 μM	Cell-free assay (3HB-GGG hydrolysis assay)	103
Caffeic acid	Phenolic acid	<i>Echinacea purpurea</i> <sup>a</sup>	IC <sub>50</sub> = 0.1 μM	Cell-free assay (HHL degradation assay)	71
Camellianin A	Flavonoid	<i>Adinandra nitida</i>	30.2% inhibition at EC of 500 μg/mL	Cell-free assay (HHL degradation assay)	102
Camellianin B	Flavonoid	<i>Adinandra nitida</i>	40.7% inhibition at EC of 500 μg/mL	Cell-free assay (HHL degradation assay)	102
Carlinoside	Flavonoid glycoside	<i>Desmodium styracifolium</i>	IC <sub>50</sub> = 33.6 μM	Cell-free assay (HHL degradation assay)	104
Catechin	Flavonoid	<i>Malus domestica</i> <sup>(a)</sup>	IC <sub>50</sub> = 109 μM	Cell-free assay (HHL degradation assay)	105
Chlorogenic acid	Phenolic acid	<i>Echinacea purpurea</i> <sup>(a)</sup>	IC <sub>50</sub> = 0.1 μM	Cell-free assay (HHL degradation assay)	71
Chrysin	Flavonoid	<i>Malus domestica</i> <sup>(a)</sup>	IC <sub>50</sub> = 146 μM	Cell-free assay (HHL degradation assay)	105
Chrysoeriol	Flavonoid	<i>Tamarix hohenackeri</i>	57.6% inhibition at EC of 20 mg/mL	Cell-free assay (HHL degradation assay)	99
Coretincone	Phenolic glycoside	<i>Coreopsis tinctoria</i>	IC <sub>50</sub> = 228 μM	Cell-free assay (HHL degradation assay)	106
Curcumin	Polyphenol	<i>Curcuma longa</i> <sup>(a)</sup>	76.9% inhibition at EC of 10 μM	Cell-free assay (HHL degradation assay)	107
Cyanidin-3-O-glucoside	Flavonoid glycoside	<i>Malus domestica</i> <sup>(a)</sup>	IC <sub>50</sub> = 174 μM	Cell-free assay (HHL degradation assay)	105

Table 1 (continued)

Compound	Class	Source	Biological action/Efficacy	Experiment	Reference
Cyanidin-3-O-galactoside	Flavonoid glycoside	<i>Malus domestica</i> <sup>(a)</sup>	IC <sub>50</sub> = 206 μM	Cell-free assay (HHL degradation assay)	105
Cyanidin-3-O-rhamnoside	Flavonoid glycoside	<i>Malus domestica</i> <sup>(a)</sup>	IC <sub>50</sub> = 114 μM	Cell-free assay (HHL degradation assay)	105
Cyanidin-3-O-sambubioside	Flavonoid glycoside	<i>Hibiscus sabdariffa</i>	IC <sub>50</sub> = 117.7 μM	Cell-free assay (FAPGG degradation assay)	108
Cyanidin-3-O-β-glucoside	Flavonoid glycoside	<i>Rosa damascena</i>	IC <sub>50</sub> = 138.8 μM	Cell-free assay (HHL degradation assay)	109
Decursidin	Coumarin	<i>Angelica decursiva</i>	IC <sub>50</sub> = 20 μM	Cell-free assay (FAPGG degradation assay)	100
(+)-trans-Decursidinol	Coumarin	<i>Angelica decursiva</i>	IC <sub>50</sub> = 4.7 μM	Cell-free assay (FAPGG degradation assay)	100
Decursinol	Coumarin	<i>Angelica decursiva</i>	IC <sub>50</sub> = 18.3 μM	Cell-free assay (FAPGG degradation assay)	100
Delphinidin-3-O-sambubioside	Flavonoid glycoside	<i>Hibiscus sabdariffa</i>	IC <sub>50</sub> = 141.6 μM	Cell-free assay (FAPGG degradation assay)	108
Epicatechin	Flavonoid	<i>Malus domestica</i> <sup>(a)</sup>	IC <sub>50</sub> = 73 μM	Cell-free assay (HHL degradation assay)	105
Gallic acid	Phenolic acid	<i>Tamarix hohenackeri</i>	43.1% inhibition at EC of 20 mg/mL	Cell-free assay (HHL degradation assay)	99
Gluco-aurantioobtusin	Antraquinone glycoside	<i>Cassia tora</i>	IC <sub>50</sub> = 30.2 μM	Cell-free assay (FAPGG degradation assay)	110
(+)-Hopeaphenol	Stilbenoid	<i>Ampelopsis brevipedunculata</i> var. <i>hancei</i>	IC <sub>50</sub> = 1.6 μM	Cell-free assay (HHL degradation assay)	72
Isoferulic acid	Phenolic acid	<i>Tamarix hohenackeri</i>	30.6% inhibition at EC of 20 mg/mL	Cell-free assay (HHL degradation assay)	99
Isoquercetrin	Flavonoid	<i>Tropaeolum majus</i> <sup>(a)</sup>	Reduced plasmatic ACE activity in SHR rats (43% inhibition at EC of 10 mg/kg)	Cell-free assay (HHL degradation assay)	111
Isorutarine	Coumarin	<i>Angelica decursiva</i>	IC <sub>50</sub> = 68.4 μM	Cell-free assay (FAPGG degradation assay)	100
Junipediol A-8-O-β-d-glucoside	Phenylpropanoid glycoside	<i>Apium graveolens</i>	IC <sub>50</sub> = 210 μM	Cell-free assay (HHL degradation assay)	112
(S)-Malic acid 1'-O-β-gentiobioside	Organic acid glycoside	<i>Lactuca sativa</i>	IC <sub>50</sub> = 27.8 μM	Cell-free assay (HHL degradation assay)	113
Mangiferin	Xanthone glycoside	<i>Swertia chirayita</i> <sup>(a)</sup>	31.5% inhibition at EC of 500 μM	Cell-free assay (HHL degradation assay)	114
Miquelianin	Flavonoid glycoside	<i>Cuphea glutinosa</i>	32.1% inhibition at EC of 100 ng/mL	Cell-free assay (FAPGG degradation assay)	115
N <sup>1</sup> ,N <sup>4</sup> ,N <sup>8</sup> -tris (dihydrocaffeoyl) spermidine	Polyamine	<i>Solanum tomentosum</i>	IC <sub>50</sub> = 9.6 ppm	Cell-free assay (3HB-GGG hydrolysis assay)	116
Methyl gallate	Phenolic acid	<i>Tamarix hohenackeri</i>	35.7% inhibition at EC of 20 mg/mL	Cell-free assay (HHL degradation assay)	99
Naringenin	Flavonoid	<i>Malus domestica</i> <sup>(a)</sup>	IC <sub>50</sub> = 78 μM	Cell-free assay (HHL degradation assay)	105
Onopordia	Polyphenol	<i>Onopordum acanthium</i> L.	IC <sub>50</sub> = 300 μM	Cell-free assay (HHL degradation assay)	117,118
Orotic acid	Organic acid	<i>Daucus carota</i> <sup>(a)</sup>	40.3% inhibition at EC of 5 μg/mL	Cell-free assay (HHL degradation assay)	119
Pd-C-I	Coumarin	<i>Angelica decursiva</i>	IC <sub>50</sub> = 6.8 μM	Cell-free assay (FAPGG degradation assay)	100
Pd-C-II	Coumarin	<i>Angelica decursiva</i>	IC <sub>50</sub> = 12.4 μM	Cell-free assay (FAPGG degradation assay)	100
Pd-C-III	Coumarin	<i>Angelica decursiva</i>	IC <sub>50</sub> = 15.3 μM	Cell-free assay (FAPGG degradation assay)	100
Quercetin	Flavonoid	<i>Malus domestica</i> <sup>(a)</sup>	IC <sub>50</sub> = 151 μM	Cell-free assay (HHL degradation assay)	105
		<i>Tamarix hohenackeri</i>	48.6% inhibition at EC of 20 mg/mL	Cell-free assay (HHL degradation assay)	99
Quercetin-3-O-galactoside	Flavonoid glycoside	<i>Malus domestica</i> <sup>(a)</sup>	IC <sub>50</sub> = 180 μM	Cell-free assay (HHL degradation assay)	105
Quercetin-3-O-glucoside	Flavonoid glycoside	<i>Malus domestica</i> <sup>(a)</sup>	IC <sub>50</sub> = 71 μM	Cell-free assay (HHL degradation assay)	105
Quercetin-3-O-glucuronic acid	Flavonoid conjugate	<i>Malus domestica</i> <sup>(a)</sup>	IC <sub>50</sub> = 27 μM	Cell-free assay (HHL degradation assay)	105
Quercetin-3-O-rhamnoside	Flavonoid glycoside	<i>Malus domestica</i> <sup>(a)</sup>	IC <sub>50</sub> = 100 μM	Cell-free assay (HHL degradation assay)	105
Quercetin-3-O-rutinoside	Flavonoid glycoside	<i>Malus domestica</i> <sup>(a)</sup>	IC <sub>50</sub> = 90 μM	Cell-free assay (HHL degradation assay)	105
Quercetin-3-O-sulfate	Flavonoid conjugate	<i>Malus domestica</i> <sup>(a)</sup>	IC <sub>50</sub> = 131 μM	Cell-free assay (HHL degradation assay)	105
Quercetin-4'-O-glucoside	Flavonoid glycoside	<i>Malus domestica</i> <sup>(a)</sup>	IC <sub>50</sub> = 211 μM	Cell-free assay (HHL degradation assay)	105
Schaftoside	Flavonoid glycoside	<i>Desmodium styracifolium</i>	IC <sub>50</sub> = 58.4 μM	Cell-free assay (HHL degradation assay)	104

(continued on next page)



Table 1 (continued)

Compound	Class	Source	Biological action/Efficacy	Experiment	Reference
Tannic acid	Phenolic acid	<i>Camellia sinensis</i> <sup>(a)</sup>	IC <sub>50</sub> = 230 μM	Cell-free assay (HHL degradation assay)	120
Taxifolin	Flavonoid	<i>Coreopsis tinctoria</i>	IC <sub>50</sub> = 145.7 μM	Cell-free assay (HHL degradation assay)	106
Vicenin 1	Flavonoid glycoside	<i>Desmodium styracifolium</i>	IC <sub>50</sub> <sup>a</sup> 52.5 μM	Cell-free assay (HHL degradation assay)	104
Vicenin 2	Flavonoid glycoside	<i>Desmodium styracifolium</i>	IC <sub>50</sub> = 43.8 μM	Cell-free assay (HHL degradation assay)	104
Vicenin 3	Flavonoid glycoside	<i>Desmodium styracifolium</i>	IC <sub>50</sub> = 46.9 μM	Cell-free assay (HHL degradation assay)	104
(+)-ε-Viniferin	Stilbenoid	<i>Vitis thunbergii</i> var. <i>taiwanian</i>	IC <sub>50</sub> = 35.5 μM	Cell-free assay (FAPGG degradation assay)	101
(+)-Vitisin A	Stilbenoid	<i>Vitis thunbergii</i> var. <i>taiwanian</i>	IC <sub>50</sub> = 3.3 μM	Cell-free assay (FAPGG degradation assay)	101
		<i>Ampelopsis brevipedunculata</i> var. <i>hancei</i>	IC <sub>50</sub> = 1.5 μM	Cell-free assay (HHL degradation assay)	72

3HB-GGG = 3-hydroxybutyryl-Gly-Gly-Gly; AAS = Atomic absorption spectrophotometry; AO = Acridine orange; ATP = Adenosine triphosphate; DQ-BSA = Dye quenched-bovine serum albumin; EC = The effective test concentration; ELISA = Enzyme Linked Immunosorbent Assay; FAC/MS = Frontal affinity chromatography-Mass spectrometry; FAPGG = furylacryloyl-phenylalanyl-glycyl-glycine; FRET = Fluorescence resonance energy transfer; HHL = hippuryl-L-histidyl-L-leucine; IC<sub>50</sub> = The half maximal inhibitory concentration; IFA = Immunofluorescence assay; SHR = spontaneously hypertensive rat; WB = WesternBlot.

<sup>a</sup> The study used commercial products. Here provides a natural source of compound as an example.

inhibited the pseudovirus entry, possibly by interfering with the function of the S protein.<sup>30</sup>

### 3.1.2. The plasma membrane protease TMPRSS2

Recognized as a host trypsin-like serine protease, TMPRSS2 highly expressed in alveolar cells has been demonstrated to facilitate viral entry by priming of viral S protein. Inhibition of TMPRSS2 activity could prevent infection of coronaviruses including MERS-CoV, SARS-CoV and SARS-CoV-2.<sup>31</sup> Now, several synthetic drugs like camostat mesylate, nafamostat mesylate and bromhexine which are serine protease inhibitors showed potential to inhibit SARS-CoV-2 infection.<sup>32–34</sup> However, on the side of natural products, only few compounds were reported. Xanthoangelol G isolated from *Angelica keiskei* was reported to inhibit a trypsin-like serine protease with its IC<sub>50</sub> value of 51.6 μM.<sup>35</sup> Notably, *in vitro* cell-based and *in vivo* experiments are needed to be done for the development of anti-SARS-CoV-2 drugs.

### 3.1.3. The endocytic machinery

Clathrin-mediated endocytosis has been recognized as the primary cell entry route for multiple coronaviruses, including new emerging SARS-CoV-2, by utilizing the binding of viral S protein to host receptor ACE2 molecule.<sup>36</sup> After endocytosis into the target cell, the viral particle undergoes the cleavage of S protein mediated by a pH-dependent cysteine protease cathepsin L at an acidic endolysosomal pH (~3.0–6.5), which finally triggers membrane fusion between virus and endosome, followed by release of viral genetic material into the cytoplasm. Hence, targeting endocytic pathway-associated proteins are considered to be one of promising strategies for inhibiting SARS-CoV-2 entry.<sup>37</sup> Following this idea, Table 1 summarizes natural compounds that have been reported with inhibitory effects on the vacuolar-type H<sup>+</sup>-ATPase (V-ATPase) activity, the expression and activity of cathepsins, or an increasing effect on lysosomal pH, which lead to impaired acidification and protein degradation of intracellular vesicles like endolysosome. Our search revealed that terpenes/terpenoids<sup>38–41</sup> and alkaloids<sup>42–44</sup> are two major classes of compounds acting through this strategy. In addition to individual compounds, some crude plant extracts have shown their potential for being developed as an anti-COVID-19 drug. The traditional Japanese herbal formulation named Maoto, prepared from a mixture of four plants (*Ephedrae herba*,

*Armeniaca semen*, *Cinnamomi cortex* and *Glycyrrhizae radix*), was recently shown to inhibit endolysosomal acidification.<sup>45</sup> Zhuang et al. also demonstrated that butanol crude fraction from *C. cortex* was able to inhibit the clathrin-dependent endocytosis pathway as well as the infection of SARS-CoV using cell-based assays.<sup>46</sup>

## 3.2. Natural bioactive compounds targeting viral replication

### 3.2.1. The 3-chymotrypsin-like main protease (3CL<sup>pro</sup>)

The 3CL<sup>pro</sup> is an enzyme that plays important role in replication of coronaviruses. It is responsible for the cleavage of polyproteins to functional proteins. Base on the protein structures, 3CL<sup>pro</sup> of SARS-CoV and SARS-CoV-2 show similarity of amino acid sequence at 96%, and both enzymes exhibit high conservation of active residues.<sup>47</sup> Therefore, small molecules with SAR-CoV 3CL<sup>pro</sup> inhibitory activity may also inhibit 3CL<sup>pro</sup> of SARS-CoV-2. Numerous studies have revealed for plant and mushroom derived natural compounds that could suppress SARS-CoV replication by blocking 3CL<sup>pro</sup> activity with IC<sub>50</sub> range from 8.3 to 92.4 μM in either cell-free or cell-based assays. Among them, hesperetin, a phenolic compound isolated from *Isatis indigotica* root exhibited the greatest inhibitory activity against SARS-CoV 3CL<sup>pro</sup> (IC<sub>50</sub> = 8.3 μM) in an African green monkey kidney (Vero) cell line and this effective dose did not toxic to the cells (CC<sub>50</sub> = 2.7 mM).<sup>48</sup> Other phytochemical classes that have shown promise in the inhibition of this enzyme are lignoid, terpenoid, tanshinone and chalcone with IC<sub>50</sub> less than 25 μM.<sup>35,49–51</sup> Interestingly, the lignoid savinin was able to reduce both viral replication (Selective index > 667) and cytopathic effect on SARS-CoV-infected Vero E6 cells.<sup>49</sup> The summary of bioactive compounds against SARS-CoV 3CL<sup>pro</sup> inhibitory activity is tabulated in Table 1. Regarding to the similarity between 3CL<sup>pro</sup> of SARS-CoV and SARS-CoV-2, these natural compounds are interesting substances to screen as inhibitors of SARS-CoV-2 3CL<sup>pro</sup> activity furthermore.

### 3.2.2. The papain-like protease (PL<sup>pro</sup>)

Similar to 3CL<sup>pro</sup>, the function of PL<sup>pro</sup> is essential for coronavirus replication by generating RTC through proteolytic processing of viral polyprotein. Hence, PL<sup>pro</sup> could be served as another attractive target of drug discovery for treatment of coronavirus infection, especially SARS-CoV-2. At present, there is no FDA

**Table 2**  
List of anti-SARS-CoV compounds from natural sources with unidentified mechanism of action.

Compound	Class	Source	Biological action/Efficacy	Experiment	Reference
Cinnamtannin B1	Flavonoid	<i>Cinnamomi cortex</i>	IC <sub>50</sub> = 32.9 μM (HIV/SARS-CoV S pseudovirus) IC <sub>50</sub> = 32.9 μM (Wild-type SARS-CoV)	Cell-based assay (Luciferase reporter assay) Cell-based assay (Plaque reduction assay)	46
Lycorine	Crystalline alkaloid	<i>Lycoris radiata</i>	IC <sub>50</sub> = 15.7 nM	Cell-based assay (CPE/MTS assay)	121
Procyanidin A2	Flavonoid	<i>Cinnamomi cortex</i>	IC <sub>50</sub> = 120.7 μM (HIV/SARS-CoV S pseudovirus) IC <sub>50</sub> = 29.9 μM (Wild-type SARS-CoV)	Cell-based assay (Luciferase reporter assay) Cell-based assay (Plaque reduction assay)	46
Procyanidin B1	Flavonoid	<i>Cinnamomi cortex</i>	IC <sub>50</sub> = 161.1 μM (HIV/SARS-CoV S pseudovirus) IC <sub>50</sub> = 41.3 μM (Wild-type SARS-CoV)	Cell-based assay (Luciferase reporter assay) Cell-based assay (Plaque reduction assay)	46

CPE/MTS = cytopathic effect-based MTS reduction; IC<sub>50</sub> = the half maximal inhibitory concentration.

<sup>(a)</sup> The study used commercial products. Here provides a natural source of compound as an example.

approved PL<sup>PRO</sup> inhibitor available, therefore identification of bioactive compounds from medicinal plants that specifically inhibit PL<sup>PRO</sup> has been focused to develop a new class of anti-coronavirus drug. According to high similarity of protein sequences and active residues between SARS-CoV and SARS-CoV-2 PL<sup>PRO</sup> (83%),<sup>47</sup> the compounds that have been reported as inhibitors of SARS-CoV PL<sup>PRO</sup> may also be effective against SARS-CoV-2. Table 1 lists many interesting compounds from natural sources that exhibited SARS-CoV PL<sup>PRO</sup> inhibitory activity. The IC<sub>50</sub> values of the compounds ranged from 0.8 to 19.3 μM, demonstrating their strong inhibitory potential. Among them, the cryptotanshinone and tanshinone IIA were regarded as two most excellent inhibitors.<sup>51</sup>

### 3.2.3. The replication/transcription complex (RTC)

The replication of full-length genomic RNA and the discontinuous transcription of subgenomic RNA transcripts are crucial for the production of new coronavirus particles inside the host cell. Both processes are mediated by the coronavirus RTC composed of multiple viral nsps including two key replicative enzymes like the RdRp (nsp12) and helicase (nsp13),<sup>52</sup> which are now considered as potential targets for COVID-19 therapy. Considering a strikingly high homology of nucleotide sequence, amino acid sequence and protein structure between SARS-CoV and SARS-CoV-2 RdRp,<sup>53</sup> the natural compounds with previous reports of inhibitory activities towards RdRp of SARS-CoV could also have the potential to suppress the activities of those enzymes of the SARS-CoV-2. It was shown that the water extract from *Houttuynia cordata* exhibited a dose-dependent inhibition on SARS-CoV RdRp activity with the highest decrease by 74% in the treatment of 800 μg/mL.<sup>54</sup> That activity of *H. cordata* was confirmed in another study by Fung et al., along with *Sinomenium acutum*, *Coriolus versicolor*, *Ganoderma lucidum* and a traditional Chinese herbal formula Kwan Du Bu Fei Dang. Their IC<sub>50</sub> values were 251.1, 198.6, 108.4, 41.9 and 471.3 μg/mL, respectively.<sup>55</sup> The inhibitors of SARS-CoV helicase also serve as a potential drug candidate since this enzyme has a highly conserved sequence among coronaviruses and shares the similar structure to that of SARS-CoV-2.<sup>52</sup> Herein, three plant-derived bioactive compounds that could be natural inhibitors of SARS-CoV-2 helicase are listed in Table 1.

### 3.2.4. The zinc ion

Zinc is an essential micronutrient that is required for various cellular metabolic processes, not only in human immunity but also in the replication of many viruses.<sup>56</sup> Although Zinc ion (Zn<sup>2+</sup>) acts as a cofactor for several important viral enzymes such as RdRp, 3CL<sup>PRO</sup> and PL<sup>PRO</sup>, it is interesting that its high intracellular concentration was found to inhibit those enzyme activities of a variety of RNA viruses including SARS-CoV,<sup>56–58</sup> thus leading to subsequent decrease in the production of new virions. Therefore, Zn<sup>2+</sup> possesses antiviral properties through generating host immune responses and inhibiting viral replication. As of now, several

researchers have suggested the use of Zn<sup>2+</sup> ionophore, a compound that stimulates cellular import of Zn<sup>2+</sup> (e.g., chloroquine and its derivatives), as a possible option for the treatment of COVID-19.<sup>59</sup> In Table 1, we summarized some natural compounds with Zn<sup>2+</sup> ionophore activity. The most promising compound is epigallocatechin-3-gallate (EGCG), followed by quercetin, luteolin, tannic acid and resveratrol.<sup>60–62</sup>

### 3.3. Natural bioactive compounds targeting viral release

#### 3.3.1. The viroporin 3a

The viroporins are small, pore-forming, viral-encoded accessory proteins with ion channel activity that have been known to play an essential role in mediating several processes in the life cycle of many viruses, including coronaviruses.<sup>63</sup> Viroporin 3a functions are strongly involved in the regulation of viral budding and release from infected cells.<sup>13</sup> Interestingly, this protein was found unique to SARS-CoV and SARS-CoV-2 and not present in other known coronaviruses,<sup>64</sup> thus the viroporin 3a protein can be an important potential therapeutic target for COVID-19. Summary of natural compounds with inhibitory effect on viroporin 3a activity is presented in Table 1. Schwarz et al. revealed that flavonoid compounds like kaempferol and its derivatives were capable of blocking the ion channel activity of SARS-CoV viroporin 3a protein. Among them, the most potent one is the glycoside juglanine, kaempferol 3-O- $\alpha$ -L-arabinopyranoside, exhibiting IC<sub>50</sub> of 2.3 μM.<sup>65</sup> Another kaempferol glycoside tiliroside and the anthraquinone emodin also showed good inhibitory activity with and IC<sub>50</sub> of 20 μM.<sup>66</sup>

### 3.4. Natural bioactive compounds targeting inflammation-related pathogenesis

Upon binding to SARS-CoV-2 S protein, the ACE2 function is downregulated which leads to increased angiotensin II level and overactivation of the AT1R signaling, causing the deleterious effects associated with excessive inflammation on several tissues.<sup>67</sup> Therefore, suppressing angiotensin II production by ACE inhibitors and blocking of AT1R by angiotensin-receptor blockers (ARBs) may be of benefit to ameliorate Ang II/AT1R-mediated inflammation in COVID-19 patients. Moreover, it was shown that an ARB could not only reduce AT1R activation, but also activate the AT2R, thus resulting in a production of vasodilation benefit.<sup>68</sup>

Currently, ACE inhibitors and ARBs are commonly prescribed in COVID-19 patients with severe symptoms. Even though risks of the use of hypertensive drugs were concerned, accumulating evidence has not suggested the association between the drugs and worse clinical outcomes.<sup>69,70</sup> Interestingly, a great number of natural compounds have been identified as potent ACE inhibitors and ARBs. Given that there are minimal side effects of using drugs from natural sources, those compounds with potential activity should be considered and investigated. Bioactive compounds derived from

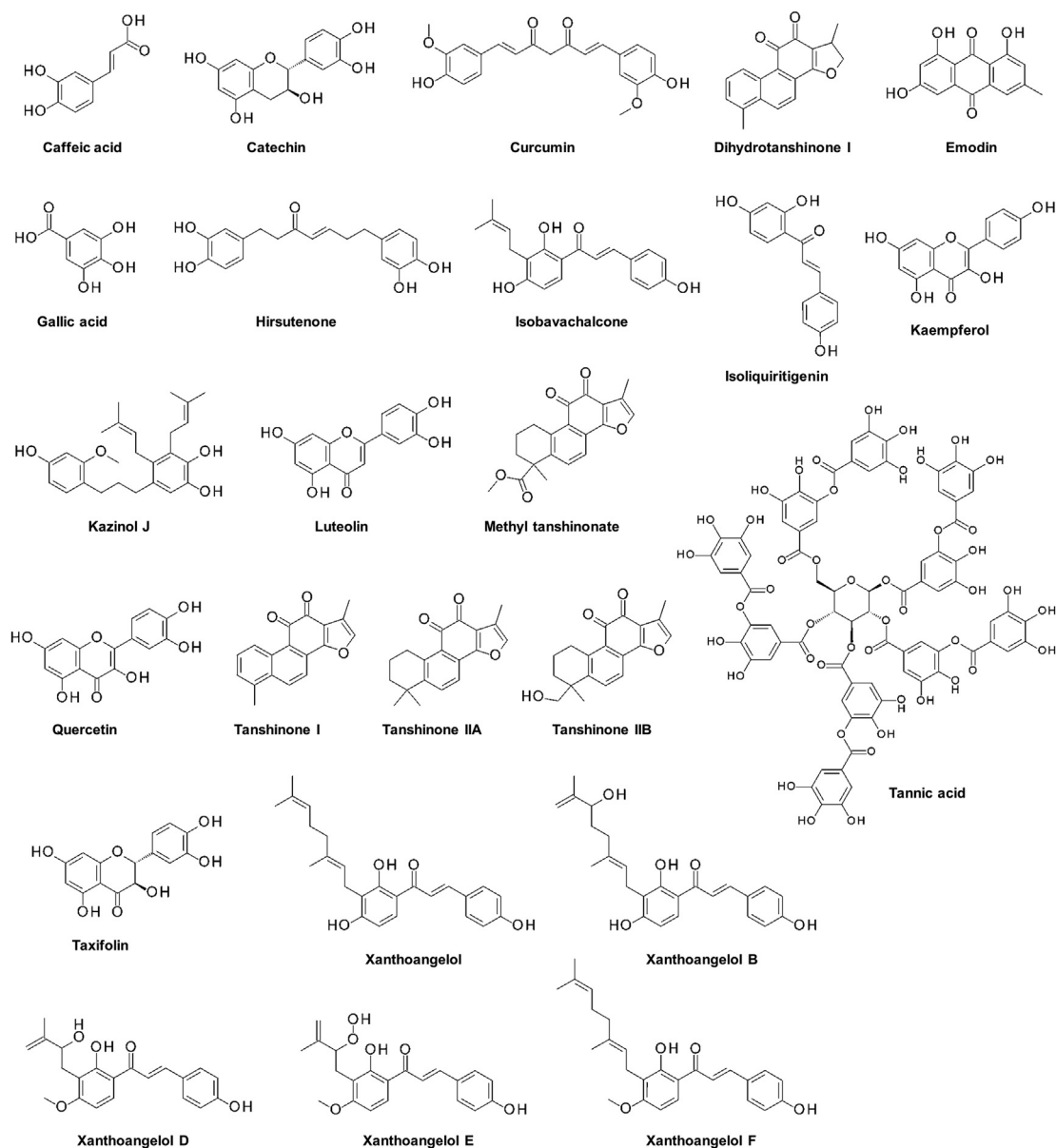


Fig. 2. Chemical structures of natural compounds with potential antiviral properties against multiple therapeutic targets for COVID-19.

natural sources which possess ACE inhibitory activity are summarized in Table 1. Among them, the excellent inhibitory properties against ACE were exerted by the phenolic caffeic acid and chlorogenic acid, and the stilbenoid hopeaphenol and vitisin A, with  $IC_{50}$  less than  $2 \mu M$ .<sup>71,72</sup> These two stilbenoids were also found to be resveratrol tetramers exhibiting multifaceted properties including anti-inflammation<sup>73</sup> and antiviral infection as a potent inhibitor of hepatitis C virus helicase.<sup>74</sup> However, only few compounds have shown the ability to block AT1R which one of them is [6]-gingerol, the major bioactive compounds present in *Zingiber officinale*. According to the report by Liu and colleagues, it could inhibit AT1R activity with  $IC_{50}$  of  $8.2 \mu M$  as detected by cell-based calcium mobilization assay.<sup>75</sup>

### 3.5. Anti-SARS-CoV natural compounds with unidentified mechanism of action

Some natural occurring compounds have been reported their

beneficial effect to inhibit SARS-CoV, even though their mechanisms of action have not yet been identified (Table 2). Accordingly, the compounds from those previous studies might also have a potency to inhibit COVID-19 infection. Using HIV/SARS-CoV S pseudovirus and wild-type SARS-CoV, three anthocyanins derived from *Cinnamomi cortex*, cinnamtannin B1, procyanidin A2 and procyanidin B1, were reported their inhibitory activities against the infection of both viruses, but at least not through the inhibition of clathrin-mediated endocytosis.<sup>46</sup> This study also investigated the effects of some crude plant extracts and found that aqueous extract of *Caryophylli Flos* exhibited moderate inhibition to pseudovirus ( $IC_{50} = 58.8 \mu M$ ) and wild-type virus ( $IC_{50} = 50.1 \mu M$ ).<sup>46</sup> In addition, the natural alkaloid lycorine, isolated from *Lycoris radiate*, has been suggested as an anti-SARS-CoV compound with an  $IC_{50}$  value of  $15.7 nM$ .<sup>121</sup>

#### 4. Conclusion and further prospects

Emerged as the most devastating viral infection in this era for the human race, the COVID-19 pandemic has introduced “new normal” for changing life as we recognize it. As numbers of new COVID-19 infected cases are rising globally, disruption of the transmission chain to minimize this spread is seriously unavoidable. This rise in COVID-19 infection is hardly disrupted unless its infective mechanisms including entry, replication and release, and modification of RAAS can be properly eliminated by humans. Certainly, we are waiting for effective strategies including drugs and vaccines to fight against COVID-19. Due to the unavailability of drugs to treat this infection, natural compounds are a main area of anti-COVID-19 research discovery. Our review suggests that 24 natural compounds have showed their potential actions on multiple therapeutic targets, which should be further explored for anti-COVID-19 plant/mushroom-based medicines (Fig. 2). The classes of these phytochemical compounds include chalcones ( $n = 7$ ), flavonoids ( $n = 5$ ), tanshinones ( $n = 5$ ), phenolic acids ( $n = 3$ ), polyphenol ( $n = 1$ ), anthraquinone ( $n = 1$ ), diarylheptanoid ( $n = 1$ ) and biphenylpropanoid ( $n = 1$ ). Among them, a natural flavonoid quercetin is found as a lead candidate with its ability on the virus side to inhibit SARS-CoV S protein-ACE2 interaction, viral protease and helicase activities, as well as on the host cell side to inhibit ACE activity and increase intracellular zinc level, thus making it very promising to reduce the disease burden. Although it is previously speculated that certain ACE inhibitors with an increased activity of ACE2 receptor may indeed enhance viral infectivity, recent studies revealed no substantial association between increased risks of infection and ACE inhibitor medications.<sup>69,70</sup> Therefore, it is worth noting that many potential mechanisms of anti-COVID-19 natural agents are required to carefully and substantially investigated. Together with proper proactive investments, it is our great hope that qualified natural compound-based medicines from promising leads described here will be developed as anti-COVID-19 soon to benefit the human race in this “new normal” era.

#### Taxonomy (classification by EVIDE)

Emerging Infectious Disease, Viral Infection of Respiratory System, Severe Acute Respiratory Syndrome Coronavirus, Cell culture, Molecular Biology, Traditional herbal medicine, Natural Product Analysis.

#### Declaration of competing interest

The authors declare that they have no conflict of interest.

#### Acknowledgments

This work was partially supported by Grant for Research, Ratchadaphiseksomphot Endowment Fund, Chulalongkorn University, Thailand.

#### References

1. Who. *Novel Coronavirus – China*; 2020. <https://www.who.int/csr/don/12-january-2020-novel-coronavirus-china/en/>. Accessed December 15, 2020.
2. Zhu N, Zhang D, Wang W, et al. A novel coronavirus from patients with pneumonia in China, 2019. *N Engl J Med*. 2020;382(8):727–733.
3. Huang C, Wang Y, Li X, et al. Clinical features of patients infected with 2019 novel coronavirus in Wuhan, China. *Lancet*. 2020;395(10223):497–506.
4. Wang D, Hu B, Hu C, et al. Clinical characteristics of 138 hospitalized patients with 2019 novel coronavirus-infected pneumonia in wuhan, China. *J Am Med Assoc*. 2020.
5. Jin YH, Cai L, Cheng ZS, et al. A rapid advice guideline for the diagnosis and treatment of 2019 novel coronavirus (2019-nCoV) infected pneumonia (standard version). *Mil Med Res*. 2020;7(1):4.
6. Singh AK, Singh A, Singh R, Misra A. Hydroxychloroquine in patients with COVID-19: a systematic review and meta-analysis. *Diabetes Metab Syndr*. 2020;14(4):589–596.
7. Taccone FS, Gorham J, Vincent JL. Hydroxychloroquine in the management of critically ill patients with COVID-19: the need for an evidence base. *Lancet Respir Med*. 2020.
8. Fuzimoto AD, Isidoro C. The antiviral and coronavirus-host protein pathways inhibiting properties of herbs and natural compounds - additional weapons in the fight against the COVID-19 pandemic? *Journal of traditional and complementary medicine*. 2020;10(4):405–419.
9. Panyod S, Ho CT, Sheen LY. Dietary therapy and herbal medicine for COVID-19 prevention: a review and perspective. *Journal of traditional and complementary medicine*. 2020;10(4):420–427.
10. Lin LT, Hsu WC, Lin CC. Antiviral natural products and herbal medicines. *Journal of traditional and complementary medicine*. 2014;4(1):24–35.
11. Wang H, Yang P, Liu K, et al. SARS coronavirus entry into host cells through a novel clathrin- and caveolae-independent endocytic pathway. *Cell Res*. 2008;18(2):290–301.
12. Song Z, Xu Y, Bao L, et al. From SARS to MERS, thrusting coronaviruses into the spotlight. *Viruses*. 2019;11(1).
13. Lu W, Zheng BJ, Xu K, et al. Severe acute respiratory syndrome-associated coronavirus 3a protein forms an ion channel and modulates virus release. *Proc Natl Acad Sci USA*. 2006;103(33):12540–12545.
14. South AM, Brady TM, Flynn JT. ACE2 (Angiotensin-Converting enzyme 2), COVID-19, and ACE inhibitor and Ang II (angiotensin II) receptor blocker use during the pandemic: the pediatric perspective. *Hypertension (Dallas, Tex.: 1979)*. 2020;76(1):16–22.
15. Shete A. Urgent need for evaluating agonists of angiotensin-(1-7)/Mas receptor axis for treating patients with COVID-19. *Int J Infect Dis : IJID : official publication of the International Society for Infectious Diseases*. 2020;96:348–351.
16. Yang J, Petitjean SJL, Koehler M, et al. Molecular interaction and inhibition of SARS-CoV-2 binding to the ACE2 receptor. *Nat Commun*. 2020;11(1):4541.
17. Lan J, Ge J, Yu J, et al. Structure of the SARS-CoV-2 spike receptor-binding domain bound to the ACE2 receptor. *Nature*. 2020;581(7807):215–220.
18. Tortorici MA, Vesler D. Structural insights into coronavirus entry. *Adv Virus Res*. 2019;105:93–116.
19. Li F, Li W, Farzan M, Harrison SC. Structure of SARS coronavirus spike receptor-binding domain complexed with receptor. *Science (New York, N.Y.)*. 2005;309(5742):1864–1868.
20. Lu L, Liu Q, Zhu Y, et al. Structure-based discovery of Middle East respiratory syndrome coronavirus fusion inhibitor. *Nat Commun*. 2014;5:3067.
21. Wu C, Liu Y, Yang Y, et al. Analysis of therapeutic targets for SARS-CoV-2 and discovery of potential drugs by computational methods. *Acta Pharm Sin B*. 2020.
22. Lu R, Zhao X, Li J, et al. Genomic characterisation and epidemiology of 2019 novel coronavirus: implications for virus origins and receptor binding. *Lancet*. 2020;395(10224):565–574.
23. Wan Y, Shang J, Graham R, Baric RS, Li F. Receptor recognition by the novel coronavirus from wuhan: an analysis based on decade-long structural studies of SARS coronavirus. *J Virol*. 2020;94(7).
24. Wrapp D, Wang N, Corbett KS, et al. Cryo-EM structure of the 2019-nCoV spike in the prefusion conformation. *Science (New York, N.Y.)*. 2020;367(6483):1260–1263.
25. Chen Y, Guo Y, Pan Y, Zhao ZJ. Structure analysis of the receptor binding of 2019-nCoV. *Biochem Biophys Res Commun*. 2020;525(1):135–140.
26. Hamming I, Timens W, Bulthuis ML, Lely AT, Navis G, van Goor H. Tissue distribution of ACE2 protein, the functional receptor for SARS coronavirus. A first step in understanding SARS pathogenesis. *J Pathol*. 2004;203(2):631–637.
27. Ashraf UM, Abokor AA, Edwards JM, et al. SARS-CoV-2, ACE2 expression, and systemic organ invasion. *Physiol Genom*. 2020.
28. The COVID-19 RISK and Treatments (CORIST) Collaboration. Use of hydroxychloroquine in hospitalised COVID-19 patients is associated with reduced mortality: findings from the observational multicentre Italian CORIST study. *Eur J Intern Med*. 2020;82:38–47.
29. Ho TY, Wu SL, Chen JC, Li CC, Hsiang CY. Emodin blocks the SARS coronavirus spike protein and angiotensin-converting enzyme 2 interaction. *Antivir Res*. 2007;74(2):92–101.
30. Yi L, Li Z, Yuan K, et al. Small molecules blocking the entry of severe acute respiratory syndrome coronavirus into host cells. *J Virol*. 2004;78(20):11334–11339.
31. McKee DL, Sternberg A, Stange U, Laufer S, Naujokat C. Candidate drugs against SARS-CoV-2 and COVID-19. *Pharmacol Res*. 2020:104859.
32. Hoffmann M, Kleine-Weber H, Schroeder S, et al. SARS-CoV-2 cell entry depends on ACE2 and TMPRSS2 and is blocked by a clinically proven protease inhibitor. *Cell*. 2020.
33. Wang M, Cao R, Zhang L, et al. Remdesivir and chloroquine effectively inhibit the recently emerged novel coronavirus (2019-nCoV) in vitro. *Cell Res*. 2020;30(3):269–271.
34. Maggio R, Gu Corsini. Repurposing the mucolytic cough suppressant and TMPRSS2 protease inhibitor bromhexine for the prevention and management of SARS-CoV-2 infection. *Pharmacol Res*. 2020.
35. Park J-Y, Ko J-A, Kim DW, et al. Chalcones isolated from *Angelica keiskei*



- inhibit cysteine proteases of SARS-CoV. *J Enzym Inhib Med Chem.* 2016;31(1):23–30.
36. Inoue Y, Tanaka N, Tanaka Y, et al. Clathrin-dependent entry of severe acute respiratory syndrome coronavirus into target cells expressing ACE2 with the cytoplasmic tail deleted. *J Virol.* 2007;81(16):8722–8729.
  37. Yang N, Shen HM. Targeting the endocytic pathway and autophagy process as a novel therapeutic strategy in COVID-19. *Int J Biol Sci.* 2020;16(10):1724–1731.
  38. Barquero AA, Alché LE, Coto CE. Block of vesicular stomatitis virus endocytic and exocytic pathways by 1-cinnamoyl-3,11-dihydroxymeliacarpin, a tetrannortriterpenoid of natural origin. *J Gen Virol.* 2004;85(Pt 2):483–493.
  39. Sun H, Huang M, Yao N, et al. The cycloartane triterpenoid ADCX impairs autophagic degradation through Akt overactivation and promotes apoptotic cell death in multidrug-resistant HepG2/ADM cells. *Biochem Pharmacol.* 2017;146:87–100.
  40. Kuzu OF, Gowda R, Sharma A, Robertson GP. Leelamine mediates cancer cell death through inhibition of intracellular cholesterol transport. *Mol Canc Therapeut.* 2014;13(7):1690–1703.
  41. Martins BX, Arruda RF, Costa GA, et al. Myrtenal-induced V-ATPase inhibition – a toxicity mechanism behind tumor cell death and suppressed migration and invasion in melanoma. *Biochim Biophys Acta Gen Subj.* 2019;1863(1):1–12.
  42. Wu MY, Wang SF, Cai CZ, et al. Natural autophagy blockers, dauricine (DAC) and dauriosoline (DAS), sensitize cancer cells to camptothecin-induced toxicity. *Oncotarget.* 2017;8(44):77673–77684.
  43. Wang Z, Zhang J, Wang Y, et al. Matrine, a novel autophagy inhibitor, blocks trafficking and the proteolytic activation of lysosomal proteases. *Carcinogenesis.* 2013;34(1):128–138.
  44. Qiu W, Su M, Xie F, et al. Tetrandrine blocks autophagic flux and induces apoptosis via energetic impairment in cancer cells. *Cell Death Dis.* 2014;5(3):e1123.
  45. Masui S, Nabeshima S, Ajsaka K, et al. Maoto, a traditional Japanese herbal medicine, inhibits uncoating of influenza virus. *Evid base Compl Alternative Med : eCAM.* 2017;2017:1062065.
  46. Zhuang M, Jiang H, Suzuki Y, et al. Procyanidins and butanol extract of Cinnamon cortex inhibit SARS-CoV infection. *Antivir Res.* 2009;82(1):73–81.
  47. Liu W, Morse JS, Lalonde T, Xu S. Learning from the past: possible urgent prevention and treatment options for severe acute respiratory infections caused by 2019-nCoV. *Chembiochem : a European journal of chemical biology.* 2020.
  48. Lin C-W, Tsai F-J, Tsai C-H, et al. Anti-SARS coronavirus 3C-like protease effects of Isatis indigotica root and plant-derived phenolic compounds. *Antivir Res.* 2005;68(1):36–42.
  49. Wen C-C, Kuo Y-H, Jan J-T, et al. Specific plant terpenoids and lignoids possess potent antiviral activities against severe acute respiratory syndrome coronavirus. *J Med Chem.* 2007;50(17):4087–4095.
  50. Liu Y-P, Cai X-H, Feng T, Li Y, Li X-N, Luo X-D. Triterpene and sterol derivatives from the roots of *Breynia fruticosa*. *J Nat Prod.* 2011;74(5):1161–1168.
  51. Park J-Y, Kim JH, Kim YM, et al. Tanshinones as selective and slow-binding inhibitors for SARS-CoV cysteine proteases. *Bioorg Med Chem.* 2012;20(19):5928–5935.
  52. Romano M, Ruggiero A, Squeglia F, Maga G, Berisio R. A structural view of SARS-CoV-2 RNA replication machinery: RNA synthesis, proofreading and final capping. *Cells.* 2020;9(5).
  53. Morse JS, Lalonde T, Xu S, Liu WR. Learning from the past: possible urgent prevention and treatment options for severe acute respiratory infections caused by 2019-nCoV. *Chembiochem : a European journal of chemical biology.* 2020;21(5):730–738.
  54. Lau KM, Lee KM, Koon CM, et al. Immunomodulatory and anti-SARS activities of *Houttuynia cordata*. *J Ethnopharmacol.* 2008;118(1):79–85.
  55. Fung KP, Leung PC, Tsui KW, et al. Immunomodulatory activities of the herbal formula Kwan Du Bu Fei Dang in healthy subjects: a randomised, double-blind, placebo-controlled study. *Hong Kong medical journal = Xianggang yi xue za zhi.* 2011;17(Suppl 2):41–43.
  56. Read SA, Obeid S, Ahlenstiel C, Ahlenstiel G. The role of zinc in antiviral immunity. *Advances in nutrition (Bethesda, Md.)* 2019;10(4):696–710.
  57. te Velthuis AJ, van den Worm SH, Sims AC, Baric RS, Snijder EJ, van Hemert MJ. Zn(2+) inhibits coronavirus and arterivirus RNA polymerase activity in vitro and zinc ionophores block the replication of these viruses in cell culture. *PLoS Pathog.* 2010;6(11), e1001176.
  58. Kaushik N, Subramani C, Anang S, et al. Zinc salts block hepatitis E virus replication by inhibiting the activity of viral RNA-dependent RNA polymerase. *J Virol.* 2017;91(21).
  59. Rahman MT, Iddid SZ. Can Zn Be a critical element in COVID-19 treatment? *Biol Trace Elem Res.* 2020:1–9.
  60. Clergeaud G, Dabbagh-Bazarbachi H, Ortiz M, Fernández-Larrea JB, O'Sullivan CK. A simple liposome assay for the screening of zinc ionophore activity of polyphenols. *Food Chem.* 2016;197(Pt A):916–923.
  61. Zhang JJ, Wu M, Schoene NW, et al. Effect of resveratrol and zinc on intracellular zinc status in normal human prostate epithelial cells. *Am J Physiol Cell Physiol.* 2009;297(3):C632–C644.
  62. Dabbagh-Bazarbachi H, Clergeaud G, Quesada IM, Ortiz M, O'Sullivan CK, Fernández-Larrea JB. Zinc ionophore activity of quercetin and epigallocatechin-gallate: from Hepa 1-6 cells to a liposome model. *J Agric Food Chem.* 2014;62(32):8085–8093.
  63. Sze CW, Tan YJ. Viral membrane channels: role and function in the virus life cycle. *Viruses.* 2015;7(6):3261–3284.
  64. Yu CJ, Chen YC, Hsiao CH, et al. Identification of a novel protein 3a from severe acute respiratory syndrome coronavirus. *FEBS Lett.* 2004;565(1-3):111–116.
  65. Schwarz S, Sauter D, Wang K, et al. Kaempferol derivatives as antiviral drugs against the 3a channel protein of coronavirus. *Planta Med.* 2014;80(2-3):177–182.
  66. Schwarz S, Sauter D, Lu W, et al. *Coronaviral Ion Channels as Target for Chinese Herbal Medicine.* vol. 3. 2012:1–13, 1.
  67. Banu N, Panikar SS, Leal LR, Leal AR. Protective role of ACE2 and its down-regulation in SARS-CoV-2 infection leading to Macrophage Activation Syndrome: therapeutic implications. *Life Sci.* 2020;256:117905.
  68. Alexandre J, Cracowski JL, Richard V, Bouhanick B. Renin-angiotensin-aldosterone system and COVID-19 infection. *Ann Endocrinol.* 2020;81(2-3):63–67.
  69. Mancia G, Rea F, Ludergrani M, Apolone G, Corrao G. Renin-angiotensin-aldosterone system blockers and the risk of covid-19. *N Engl J Med.* 2020.
  70. Reynolds HR, Adhikari S, Pulgarin C, et al. Renin-angiotensin-aldosterone system inhibitors and risk of covid-19. *N Engl J Med.* 2020.
  71. Chiou SY, Sung JM, Huang PW, Lin SD. Antioxidant, antidiabetic, and antihypertensive properties of echinacea purpurea flower extract and caffeic acid derivatives using in vitro models. *J Med Food.* 2017;20(2):171–179.
  72. Su PS, Doerkens RJ, Chen SH, et al. Screening and profiling stilbene-type natural products with angiotensin-converting enzyme inhibitory activity from *Ampelopsis brevipedunculata* var. *hancei* (Planch.) Rehder. *J Pharmaceut Biomed Anal.* 2015;108:70–77.
  73. Mi Jeong S, Davaatseren M, Kim W, et al. Vitisin A suppresses LPS-induced NO production by inhibiting ERK, p38, and NF-kappaB activation in RAW 264.7 cells. *Int Immunopharmacol.* 2009;9(3):319–323.
  74. Lee S, Yoon KD, Lee M, et al. Identification of a resveratrol tetramer as a potent inhibitor of hepatitis C virus helicase. *Br J Pharmacol.* 2016;173(1):191–211.
  75. Liu Q, Liu J, Guo H, et al. [6]-gingerol: a novel AT1 antagonist for the treatment of cardiovascular disease. *Planta Med.* 2013;79(5):322–326.
  76. He R, Shi X, Zhou M, et al. Alantolactone induces apoptosis and improves chemosensitivity of pancreatic cancer cells by impairment of autophagy-lysosome pathway via targeting TFEB. *Toxicol Appl Pharmacol.* 2018;356:159–171.
  77. Pan S, Cai H, Gu L, Cao S. Cleistanthin A inhibits the invasion and metastasis of human melanoma cells by inhibiting the expression of matrix metalloproteinase-2 and -9. *Oncology letters.* 2017;14(5):6217–6223.
  78. Zhang Z, Ma J, Zhu L, Zhao Y. Synthesis and identification of cytotoxic diphyllin glycosides as vacuolar H(+)-ATPase inhibitors. *Eur J Med Chem.* 2014;82:466–471.
  79. Chen H, Liu P, Zhang T, et al. Effects of diphyllin as a novel V-ATPase inhibitor on TE-1 and ECA-109 cells. *Oncol Rep.* 2018;39(3):921–928.
  80. Zheng K, Li Y, Wang S, et al. Inhibition of autophagosome-lysosome fusion by ginsenoside Ro via the ESR2-NCF1-ROS pathway sensitizes esophageal cancer cells to 5-fluorouracil-induced cell death via the CHEK1-mediated DNA damage checkpoint. *Autophagy.* 2016;12(9):1593–1613.
  81. Geng YD, Zhang C, Shi YM, et al. Icariside II-induced mitochondrion and lysosome mediated apoptosis is counterbalanced by an autophagic salvage response in hepatoblastoma. *Canc Lett.* 2015;366(1):19–31.
  82. Lao Y, Wan G, Liu Z, et al. The natural compound oblongifolin C inhibits autophagic flux and enhances antitumor efficacy of nutrient deprivation. *Autophagy.* 2014;10(5):736–749.
  83. Wang K, Tu Y, Wan JB, Chen M, He C. Synergistic anti-breast cancer effect of pulsatilla saponin D and camptothecin through interrupting autophagic-lysosomal function and promoting p62-mediated ubiquitinated protein aggregation. *Carcinogenesis.* 2019.
  84. Park J-Y, Yuh KJ, Ryu HW, et al. Evaluation of polyphenols from *Broussonetia papyrifera* as coronavirus protease inhibitors. *J Enzym Inhib Med Chem.* 2017;32(1):504–512.
  85. Park J-Y, Jeong HJ, Kim JH, et al. Diarylheptanoids from *Alnus japonica* inhibit papain-like protease of severe acute respiratory syndrome coronavirus. *Biol Pharm Bull.* 2012. b12-00623.
  86. Feldman M, Santos J, Grenier D. Comparative evaluation of two structurally related flavonoids, isoliquiritigenin and liquiritigenin, for their oral infection therapeutic potential. *J Nat Prod.* 2011;74(9):1862–1867.
  87. Mao Y-W, Tseng H-W, Liang W-L, Chen I-S, Chen S-T, Lee M-H. Anti-inflammatory and free radical scavenging activities of the constituents isolated from *Machilus zuihoensis*. *Molecules.* 2011;16(11):9451–9466.
  88. Chen L, Li J, Luo C, et al. Binding interaction of quercetin-3-β-galactoside and its synthetic derivatives with SARS-CoV 3CLpro: structure–activity relationship studies reveal salient pharmacophore features. *Bioorg Med Chem.* 2006;14(24):8295–8306.
  89. Cho JK, Curtis-Long MJ, Lee KH, et al. Geranylated flavonoids displaying SARS-CoV papain-like protease inhibition from the fruits of *Paulownia tomentosa*. *Bioorg Med Chem.* 2013;21(11):3051–3057.
  90. Kim DW, Seo KH, Curtis-Long MJ, et al. Phenolic phytochemical displaying SARS-CoV papain-like protease inhibition from the seeds of *Psoralea coralyfolia*. *J Enzym Inhib Med Chem.* 2014;29(1):59–63.
  91. Magro M, Campos R, Baratella D, et al. Magnetic purification of curcumin from *Curcuma longa* rhizome by novel naked maghemite nanoparticles. *J Agric Food Chem.* 2015;63(3):912–920.
  92. Bankeu JJ, Khayala R, Lenta BN, et al. Isoflavone dimers and other bioactive constituents from the figs of *Ficus mucosa*. *J Nat Prod.* 2011;74(6):1370–1378.



93. Song YH, Kim DW, Curtis-Long MJ, et al. Papain-like protease (PLpro) inhibitory effects of cinnamic amides from *Tribulus terrestris* fruits. *Biol Pharm Bull.* 2014;37(6):1021–1028.
94. Yu MS, Lee J, Lee JM, et al. Identification of myricetin and scutellarein as novel chemical inhibitors of the SARS coronavirus helicase, nsP13. *Bioorg Med Chem Lett.* 2012;22(12):4049–4054.
95. Lee C, Lee JM, Lee NR, Kim DE, Jeong YJ, Chong Y. Investigation of the pharmacophore space of Severe Acute Respiratory Syndrome coronavirus (SARS-CoV) NTPase/helicase by dihydroxochromone derivatives. *Bioorg Med Chem Lett.* 2009;19(16):4538–4541.
96. Krenn BM, Gaudernak E, Holzer B, Lanke K, Van Kuppeveld FJ, Seipelt J. Antiviral activity of the zinc ionophores pyrithione and hinokitiol against picornavirus infections. *J Virol.* 2009;83(1):58–64.
97. Schwarz S, Wang K, Yu W, Sun B, Schwarz W. Emodin inhibits current through SARS-associated coronavirus 3a protein. *Antivir Res.* 2011;90(1):64–69.
98. Chen H, Yang T, Wang MC, Chen DQ, Yang Y, Zhao YY. Novel RAS inhibitor 25-O-methylalisol F attenuates epithelial-to-mesenchymal transition and tubulointerstitial fibrosis by selectively inhibiting TGF-beta-mediated Smad3 phosphorylation. *Phytomedicine.* 2018;42:207–218.
99. Xing Y, Liao J, Tang Y, et al. ACE and platelet aggregation inhibitors from *Tamarix hohenackeri* Bunge (host plant of *Herba Cistanches*) growing in Xinjiang. *Phcog Mag.* 2014;10(38):111–117.
100. Ali MY, Seong SH, Jung HA, Choi JS. Angiotensin-I-Converting enzyme inhibitory activity of coumarins from *Angelica decursiva*. *Molecules.* 2019;24(21).
101. Lin YS, Lu YL, Wang GJ, Chen LG, Wen CL, Hou WC. Ethanolic extracts and isolated compounds from small-leaf grape (*Vitis thunbergii* var. *taiwaniana*) with antihypertensive activities. *J Agric Food Chem.* 2012;60(30):7435–7441.
102. Liu B, Yang J, Ma Y, Yuan E, Chen C. Antioxidant and angiotensin converting enzyme (ACE) inhibitory activities of ethanol extract and pure flavonoids from *Adinandra nitida* leaves. *Pharm Biol.* 2010;48(12):1432–1438.
103. Nakabayashi R, Yang Z, Nishizawa T, Mori T, Saito K. Top-down targeted metabolomics reveals a sulfur-containing metabolite with inhibitory activity against angiotensin-converting enzyme in *Asparagus officinalis*. *J Nat Prod.* 2015;78(5):1179–1183.
104. Zhang YQ, Luo JG, Han C, Xu JF, Kong LY. Bioassay-guided preparative separation of angiotensin-converting enzyme inhibitory C-flavone glycosides from *Desmodium styracifolium* by recycling complexation high-speed counter-current chromatography. *J Pharmaceut Biomed Anal.* 2015;102:276–281.
105. Balasuriya N, Rupasinghe HP. Antihypertensive properties of flavonoid-rich apple peel extract. *Food Chem.* 2012;135(4):2320–2325.
106. Wang W, Chen W, Yang Y, Liu T, Yang H, Xin Z. New phenolic compounds from *Coreopsis tinctoria* Nutt. and their antioxidant and angiotensin i-converting enzyme inhibitory activities. *J Agric Food Chem.* 2015;63(1):200–207.
107. Bhullar KS, Jha A, Youssef D, Rupasinghe HP. Curcumin and its carbocyclic analogs: structure-activity in relation to antioxidant and selected biological properties. *Molecules.* 2013;18(5):5389–5404.
108. Ojeda D, Jimenez-Ferrer E, Zamilpa A, Herrera-Arellano A, Tortoriello J, Alvarez L. Inhibition of angiotensin convertin enzyme (ACE) activity by the anthocyanins delphinidin- and cyanidin-3-O-sambubiosides from *Hibiscus sabdariffa*. *J Ethnopharmacol.* 2010;127(1):7–10.
109. Kwon EK, Lee DY, Lee H, et al. Flavonoids from the buds of *Rosa damascena* inhibit the activity of 3-hydroxy-3-methylglutaryl-coenzyme a reductase and angiotensin I-converting enzyme. *J Agric Food Chem.* 2010;58(2):882–886.
110. Hyun SK, Lee H, Kang SS, Chung HY, Choi JS. Inhibitory activities of *Cassia tora* and its anthraquinone constituents on angiotensin-converting enzyme. *Phytother Res.* 2009;23(2):178–184.
111. Gasparotto Junior A, Prando TB, Leme Tdos S, et al. Mechanisms underlying the diuretic effects of *Tropaeolum majus* L. extracts and its main component isoquercitrin. *J Ethnopharmacol.* 2012;141(1):501–509.
112. Simaratanamongkol A, Umehara K, Noguchi H, Panichayupakaranant P. Identification of a new angiotensin-converting enzyme (ACE) inhibitor from Thai edible plants. *Food Chem.* 2014;165:92–97.
113. Lagemann A, Dunkel A, Hofmann T. Activity-guided discovery of (S)-malic acid 1'-O-beta-gentiobioside as an angiotensin I-converting enzyme inhibitor in lettuce (*Lactuca sativa*). *J Agric Food Chem.* 2012;60(29):7211–7217.
114. Phoboo S, Pinto Mda S, Barbosa AC, et al. Phenolic-linked biochemical rationale for the anti-diabetic properties of *Swertia chirayita* (Roxb. ex Flem.) Karst. *Phytother Res.* 2013;27(2):227–235.
115. Santos MC, Toson NSB, Pimentel MCB, Bordignon SAL, Mendez ASL, Henriques AT. Polyphenols composition from leaves of *Cuphea* spp. and inhibitor potential, in vitro, of angiotensin I-converting enzyme (ACE). *J Ethnopharmacol.* 2020;255:112781.
116. Forero DP, Masatani C, Fujimoto Y, Coy-Barrera E, Peterson DG, Osorio C. Spermidine derivatives in lulo (*Solanum quitoense* lam.) fruit: sensory (taste) versus biofunctional (ACE-Inhibition) properties. *J Agric Food Chem.* 2016;64(26):5375–5383.
117. Salehabadi H, Khajeh K, Dabirmanesh B, Biglar M, Amanlou M. Evaluation of angiotensin converting enzyme inhibitors by SPR biosensor and theoretical studies. *Enzym Microb Technol.* 2019;120:117–123.
118. Sharifi N, Souri E, Ziai SA, Amin G, Amini M, Amanlou M. Isolation, identification and molecular docking studies of a new isolated compound, from *Onopordon acanthium*: a novel angiotensin converting enzyme (ACE) inhibitor. *J Ethnopharmacol.* 2013;148(3):934–939.
119. Hassani A, Hussain SA, Abdullah N, Kamarudin S, Rosli R. Antioxidant potential and angiotensin-converting enzyme (ACE) inhibitory activity of orotic acid-loaded gum Arabic nanoparticles. *AAPS PharmSciTech.* 2019;20(2):53.
120. Al Shukor N, Van Camp J, Gonzales GB, et al. Angiotensin-converting enzyme inhibitory effects by plant phenolic compounds: a study of structure activity relationships. *J Agric Food Chem.* 2013;61(48):11832–11839.
121. Li SY, Chen C, Zhang HQ, et al. Identification of natural compounds with antiviral activities against SARS-associated coronavirus. *Antivir Res.* 2005;67(1):18–23.